CHAPTER 9

The Development of Ocular Dominance Columns: Mechanisms and Models

K. D. Miller and M. P. Stryker

Introduction

The function of the visual cortex depends upon the precision with which its cells are connected to their inputs. Such precise connections are formed during normal development in large part by the rearrangement of initial connections whose pattern is much more diffuse. The cortical network reorganizes itself under the influence of its own neural activity.

The notion that the visual cortex is a self-organizing biological system has prompted much experimental work and theoretical interest over the past 30 years. One approach toward understanding this self-organization is to construct mathematical models of the system that incorporate the microscopic cellular properties that are believed to exist on experimental grounds. The models may then be followed, from an initial state of diffuse connectivity through a stage of refinement to an ultimate stage of precise connectivity, by computer simulation or with analytic methods. This approach can be used to determine the range of microscopic properties that can give rise to the macroscopic organization observed experimentally.

In this chapter we first present some of the experimental background to studies of the development of ocular dominance columns, a striking feature of organization of the visual cortex. We then present a formal model of the system, the elements of which correspond to identified neural structures whose relevant properties may be measured experimentally (and have been measured in adult animals). We show that several different biologically reasonable

mechanisms of synaptic plasticity may be described by the same mathematics. These mechanisms are distinguished by the different biological features that are summarized in each term of the mathematical model.

The model develops patterns like those observed in biological development. Analysis of the model allows prediction of the size of ocular dominance columns from potential experimental measurements. This analysis illuminates the relative importance of the properties of the cortex and its inputs in determining this size. The determinants of development in the model are illustrated through simulation and mathematical analysis. Finally, we outline ways in which a combination of theoretical and experimental approaches can be used to further our understanding of neural development.

Development of Ocular Dominance Columns in Visual Cortex

The primary visual cortex contains a single map of the world as seen through the two eyes. At a scale of half a millimeter, however, this map is not continuous. Instead, in adult humans, monkeys, cats, and many other species, inputs serving the two eyes are largely (or in some species completely) segregated into alternate patches serving the left and right eyes.

"Ocular dominance patches" or "columns" are the names given to these alternate patches or stripes of input serving the two eyes (figure 1). The profound influence of neural activity on their development and plasticity makes them an excellent model system for studies of the organization of connections in the central nervous system. This influence was first noted in the clinic more than 100 years ago (von Senden, 1960). At that time, it became possible to remove cataracts, which obscure vision by purely optical means, without any direct effect on the neurons of the retina. In patients who acquired cataracts in adulthood, this operation "miraculously" restored sight. In patients with congenital cataracts in one eye, that had occluded vision from the

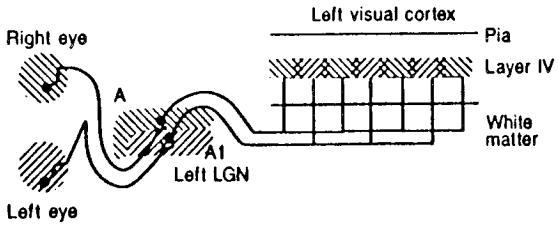

Figure 1: Cartoon showing part of the organization of the mammalian visual system. The two eyes are illustrated to the left, from which emerge the optic nerves. At the optic chiasm the fibers from the nasal side of each retina cross to the opposite optic tract en route to the lateral geniculate nucleus (LGN). The LGN receives these inputs from the two eyes in separate layers (cartooned as layers A and A1 as in the cat) and relays this visual information to the visual cortex, also known as striate cortex or area 17. In the visual cortex, terminations from the lateral geniculate nucleus are found principally in layers IV and VI, with the major concentration in layer IV. In adult animals, as illustrated, these terminals are made in eye-specific patches with a repeat distance (from the middle of one left-eye patch through the right-eye patch back to the middle of the next left-eye patch) of about a millimeter (850 um in the cat). Above and below each ocular dominance patch in layer IV, cortical neurons tend to respond better to the eye that provides input to the patch than to the other eye, revealing a columnar (vertical) organization of ocular dominance throughout all layers of the cortex; hence the name "ocular dominance columns".

time of birth, the same operation did not restore useful vision to that eye. This was true even though no serious histological damage was evident in the retina or in visual structures in the brain.

The changes in the visual system that underly this puzzling phenomenon of *amblyopia ex anopsia* (poor vision in one eye resulting from not seeing through that eye during early life), confirmed in further clinical studies, were finally explained in the early 1960s by the work of Hubel and Wiesel. They showed that most neurons in the cat's visual cortex ordinarily respond to stimulation through either eye, although perhaps one quarter of neurons respond only to a single eye (Hubel and Wiesel, 1962). Such binocular responses in the visual cortex were unchanged by even years of unilateral visual deprivation in adult animals; but as little as a few days or weeks of monocular visual deprivation during a sensitive period in early life left most cortical neurons unresponsive to the eye

whose vision had been occluded (Hubel and Wiesel, 1970; Wiesel and Hubel, 1963a). In these animals, the two eyes were entirely normal, and neurons in the lateral geniculate nucleus (LGN, see figure 1), the nucleus that is the major source of input to visual cortex, appeared to be nearly normal. The geniculate neurons in the layer driven by the deprived eye responded almost identically to those in the layer driven by the seeing eye, although they were a bit smaller and stained somewhat more palely (Wiesel and Hubel, 1963b). Thus, it appeared that neonatal monocular visual deprivation had produced a change in the visual cortex, where inputs from the two eyes first had the opportunity to interact on single neurons, but not in earlier, more peripheral stages of the visual system. Binocular visual deprivation (closure of both eyes) in early life produced no ill effects, suggesting that the changes produced by unilateral visual deprivation were due to a competitive interaction between the geniculocortical afferents serving the two eyes, rather than merely to disuse of the occluded eye's afferents (Wiesel and Hubel, 1965). This conclusion was reinforced by failure of monocular deprivation to produce changes either in the most peripheral portion of the visual field, which is viewed through only one eye, or in a region of LGN and visual cortex in which input from the seeing eye was experimentally removed (Guillery, 1972; Sherman et al., 1974).

The changes of binocular connections in the developing visual cortex appeared to be due entirely to alterations of the spatial and temporal patterns of neural discharge in geniculocortical afferents, rather than to metabolic or surgical complications of the deprivation procedure. The monocular deprivation effects did not depend on light deprivation, since similar effects were produced when the image seen by one eye was merely blurred (Wiesel and Hubel, 1963a). Perhaps the most striking finding was that when neural activity during early life was made equal but asynchronous in the two eyes by occlusion of each eye on alternate days, or by surgically or optically misaligning images in the two eyes, the partial segregation of visual responses into ocular dominance columns was made nearly complete (Hubel and Wiesel, 1965; Van Sluyters and Levitt, 1985). In such a cortex nearly all cells in each cortical column were driven exclusively by a single eye, and the eye that dominated alternated from column to column. This is in contrast to the normal case in which most neurons respond to stimulation through either eye, although cells in each column tend

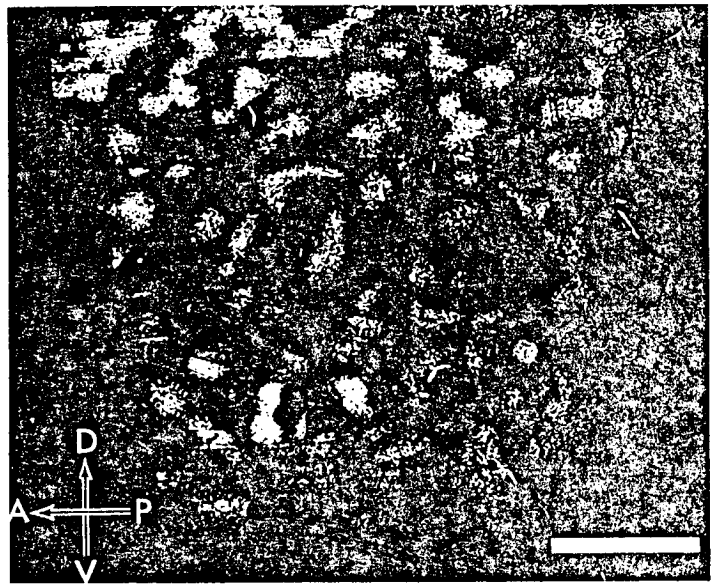

Figure 2: Surface view of ocular dominance patches in a normal cat. This is a reconstruction made from serial autoradiographically labeled parasagittal sections of layer IV of visual cortex, photographed in dark field following an injection of [^{3}H]-amino acid into one eye. Silver grains indicating the presence of geniculocortical afferent terminals serving the injected eye appear as white dots. This picture shows what the ocular dominance patches of one eye would look like if one were to flatten the cortex, remove the superficial layers, and look down on the flattened layer IV from above the cortical surface. The injected eye was ipsilateral to the cortical hemisphere shown. Scale bar = 2 mm. From LeVay, Stryker, and Shatz, 1978. Reprinted by permission of the Journal of Comparative Neurology.

to respond more strongly to stimulation through one eye than through the other (Hubel and Wiesel, 1965). This complete segregation of responses appeared not to result from alterations in levels of activity but merely from alterations in the relative timing of activity in the two eyes.

The structural basis of ocular dominance columns was revealed in experiments in which the population of geniculocortical afferent terminals serving one eye was labelled, either by degeneration methods or autoradiographically by transneuronal axonal transport of [^{3}H]-sugars or amino acids injected into the vitreous humor of one eye

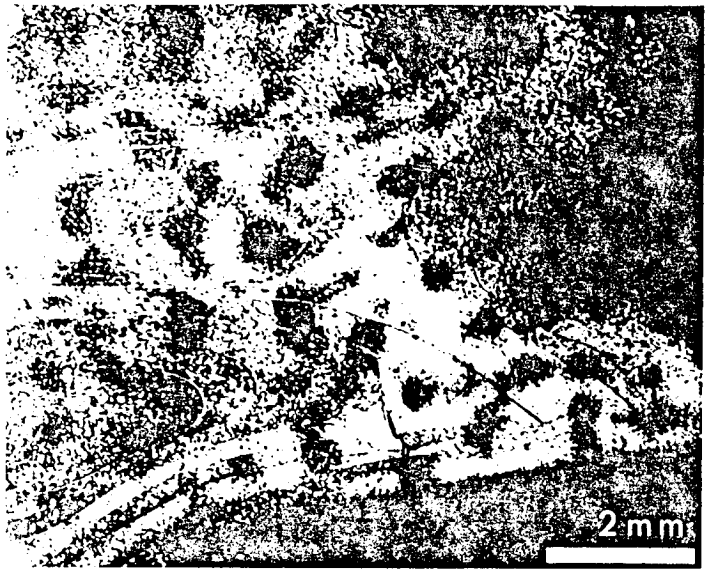

Figure 3: Surface view of ocular dominance patches in a one-year old cat that had experienced monocular visual occlusion beginning before the time of natural eye opening. The eye that had remained open during early life received an injection of [^{3}H]-amino acid. This reconstruction of the cortical hemisphere ipsilateral to the injected eye was made like that of figure 2, to which it should be compared. In these deprived animals, white dots of label indicate terminals serving the eye that had remained open. These open-eye terminals occupy more than 80 percent of layer IV. Physiological experiments in this and similar animals revealed that input from the deprived eye was confined to the holes in this sea of label. Unpublished data from experiments reported in Shatz and Stryker, 1978.

(figure 2; Hubel and Wiesel, 1972; Shatz, Lindstrom, and Wiesel, 1977; Wiesel, Hubel, and Lam, 1974). These methods demonstrated that the geniculate terminals from each eye in normal adult animals were segregated into alternate patches in layer 4 of visual cortex. These methods also revealed that an effect of early monocular deprivation was to change the relative sizes of the patches of inputs to visual cortex serving the two eyes, while keeping the repeat distance the same (figure 3) (Hubel, Wiesel, and LeVay, 1977; Shatz and Stryker, 1978). But the reason for such a sensitive period in early life, in which such small alterations in visual experience as closure of one

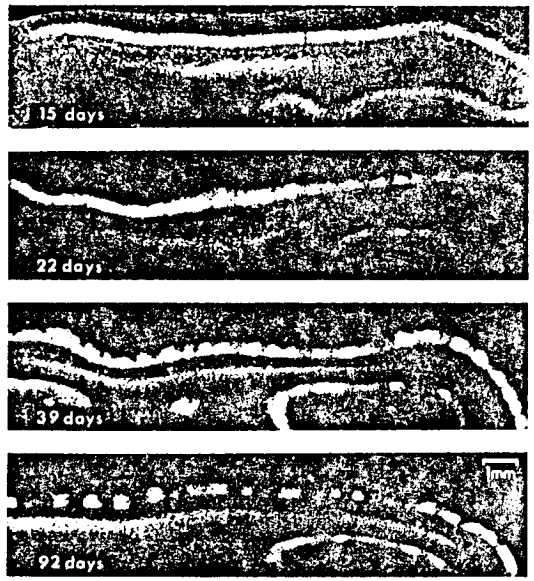

Figure 4: Progressive changes in the transneuronal labelling pattern of visual cortex following an injection of [^{3}H]-amino acid into one eye. Before 15 days of age, label from each eye is found uniformly throughout layer IV. By 21 days, periodicity in the labelling is first evident as afferents begin to segregate. The segregation proceeds rapidly until 5-6 weeks of age and more slowly thereafter, attaining nearly adult levels by 2 months and fully adult levels by 3 months of age. From LeVay and Stryker, 1979. Reprinted with permission from the Society for Neuroscience.

eye for a few days lead to permanent alterations in connectivity, remained obscure.

The reason for this early plasticity was clarified only when it was appreciated that the initial growth of eye-specific inputs into the visual cortex does not take place in the form of ocular dominance patches. Instead, geniculocortical relay cells serving the two eyes initially make connections to the cortex in a uniform, continuous, and completely overlapping fashion (Hubel, Wiesel, and LeVay, 1977; LeVay, Wiesel, and Hubel, 1980; LeVay, Stryker, and Shatz, 1978; Rakic, 1977). Ocular dominance patches then develop by the progressive segregation of these initially overlapping inputs. This development was most clearly revealed by the progressive changes in the transneuronal labelling pattern of visual cortex following an

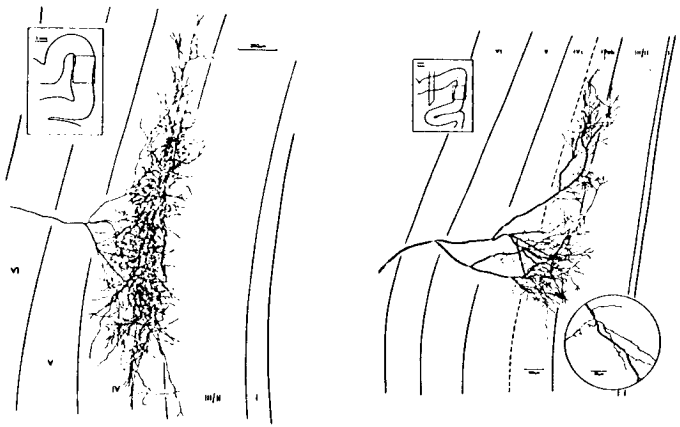

Figure 5: Presumed geniculocortical afferent terminal arbors labelled (left) by a Golgi method in an 8-day-old kitten, before the segregation of ocular dominance patches, and (right) in a normal adult cat by horseradish peroxidase injected into the optic radiations below visual cortex. Each picture shows a large afferent arbor ramifying dorsally in layer IV, presumed to be a Y-type geniculocortical afferent. Note that the arbor in the young animal is continuous over more than 2 mm, while terminals of the arbor from the adult animal are largely confined to two dense, half-millimeter patches separated by a half-millimeter space. Terminal arbors like the one shown from the young animal are not found in adults, and presumably must be "pruned" (or lost) during normal development. Left: from LeVay and Stryker, 1979. Reprinted with permission from the Society for Neuroscience. Right: from Ferster and LeVay, 1978. Reprinted by permission of the Journal of Comparative Neurology.

injection into one eye of animals at different ages (figure 4).

At least some of the early geniculocortical connections are from afferents that arborize over more than 2 mm in cortex, a distance large enough to span two pairs of ocular dominance columns (LeVay and Stryker, 1979) (figure 5). Beginning prenatally in humans and monkeys, but postnatally in cats, these afferents reorganize their terminal arbors so as to partition the cortex into the alternate, half-millimeter ocular dominance patches. It is only during and slightly after this period in which geniculocortical connections are normally reorganizing that they are sensitive to monocular deprivation. Thus, we may interpret the plasticity produced by monocular deprivation not as a bizarre pathological response, but as the abnormal outcome, produced by abnormal patterns of activity, of a normal developmental

process.

A mechanism similar to that described by Hebb (1949) was proposed to account for these phenomena produced by visual deprivation during early life (Changeux and Danchin, 1976; Stent, 1973). The Hebb rule postulates that synapses are strengthened to the extent that the activities of pre- and postsynaptic neurons are correlated and that synapses are weakened otherwise. Thus, correlated patterns of inputs would compete for the ability to activate a postsynaptic cell: the synapses corresponding to the pattern that best activated the cell would be strengthened, and other synapses correspondingly weakened. If afferents representing a single eye are better correlated with one another than with afferents of the opposite eye, inputs representing the two eyes would compete with one another in cortex. The outcome of such competition could be altered by alteration of the activity patterns of the two eyes. The experiments

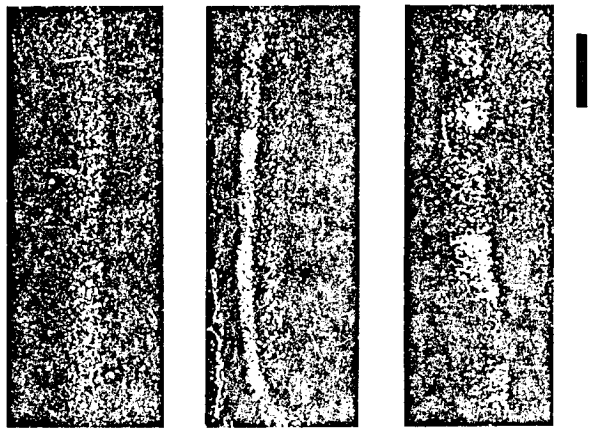

Figure 6: Ocular dominance columns in 7-10 week old TTX-treated (l), dark-reared (c), and control animals (r) labelled autoradiographically as in figures 2-4. Note that ocular dominance patches are absent in the animal in which all retinal activity had been blocked with TTX, so that this animal resembles the youngest animal shown in figure 4. Note also that ocular dominance patches are present in the animals that were reared in darkness. Although these dark-reared animals lacked visual experience, spontaneous neuronal discharge in the retinae was unblocked. Scale bar = 1 mm. Unpublished data from experiments reported in Stryker and Harris, 1986.

described thus far demonstrate that alterations in visual experience interfere with the normal process of geniculocortical afferent segregation. They do not, however, reveal whether neural activity is necessary for normal segregation, as would be the case if the Hebb mechanism were responsible. To investigate this question, Stryker and Harris (1986) blocked neural activity in the two eyes by repeated intraocular injections of the voltage-sensitive sodium channel ligand, tetrodotoxin (TTX), during the period in which ocular dominance columns normally develop. In such animals, neural activity was dramatically reduced in LGN and visual cortex, and geniculocortical afferents did not form ocular dominance patches; they remained instead in their infantile state of complete overlap (figure 6). This lack of segregation was also apparent physiologically in neuronal response properties. In normal animals, many neurons are driven exclusively through one eye or the other, as shown in figure 7 (left). In contrast, in TTX-treated animals nearly all neurons in the cortex were driven well through both eyes, as shown in figure 7 (right).

These experiments suggested that the normal developmental rearrangement of geniculocortical synaptic connections to form ocular dominance columns required neural activity. Since ocular dominance columns form, to a considerable extent, in utero in the monkey (DesRosiers et al., 1978; LeVay, Wiesel, and Hubel, 1980; Rakic, 1977), and in cats reared with bilateral lid suture or in total darkness, it appears that the so-called "spontaneous" or maintained activity of retinal ganglion cells in darkness is sufficient for segregation and that visually driven activity is not required.

The maintained activity of retinal ganglion and geniculate cells in darkness has been investigated in adult cats and in other species. Neighboring ganglion cells of the same center type tend to fire together over time periods of a millisecond to a few tens of milliseconds, and this correlation of activity decreases with increasing distance across the retina (Mastronarde, 1983a,b). In addition, correlations over longer time scales of activities within each eye or each lamina of the LGN are also present (Levick and Williams, 1964; Rodieck and Smith, 1966). With such correlated activity, a Hebb rule for the adjustment of geniculocortical synaptic strengths would be expected to allow the geniculocortical afferents serving each eye to remain together, while lack of correlation between activity in the two eyes causes the two eyes' afferents to segregate from one another.

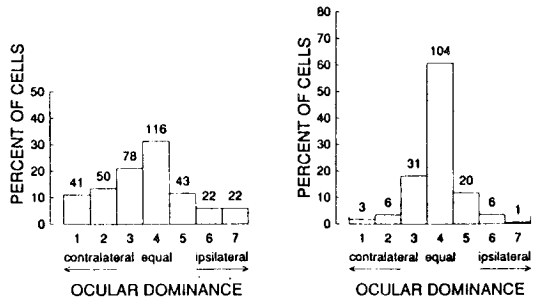

Figure 7: Ocular dominance histograms from visually responsive single units in the visual cortex of 6 normal kittens, 36 to 51 days of age (left) or of four kittens subject to bilateral retinal activity blockade by injection of TTX (right). Histograms plot percentage of units in each of 7 ocular dominance groups defined by Hubel and Wiesel (1962): group 1 (7) for units driven exclusively by contralateral (ipsilateral) eye; group 2 (6) for units strongly dominated by contralateral (ipsilateral) eye; group 3 (5) for units weakly dominated by contralateral (ipsilateral) eye; and group 4 for units driven nearly equally through the 2 eyes. Number of units in each bar of histograms is indicated above bar. Left: Normal kittens. Note that many neurons are driven well by both eyes but that a large fraction are strongly dominated or exclusively driven by one eye or the other (groups 1-2 and 6-7). Right: Kittens subject to bilateral retinal activity blockade. Retinal activity was blockaded beginning at age 14-16 days, and continuing through age 39-57 days. Kittens were allowed to recover from blockade for 2-4 days before microelectrode recording. Note the increased percentage of cells driven well by either eye (groups 3-5). These and the following histograms include cells from the cortical layers above and below layer IV, as well as from within layer IV. In normal animals there is a greater degree of binocular mixing in the layers other than layer IV. Data replotted from experiments reported in Stryker and Harris, 1986.

We have carried out several tests of assumptions implicit in the Hebb-synapse explanation of ocular dominance column development. One basic assumption is that the neural activity relevant to plasticity was the activity in the visual cortex. The experiments described thus far had all interfered with activity at earlier stages of the visual system as well. We tested this assumption by infusing TTX into a region of cortex to block the discharge of cortical cells and their geniculocortical afferent terminals (Reiter, Waitzman and Stryker, 1986). We then instituted a period of monocular deprivation and studied whether this deprivation caused a

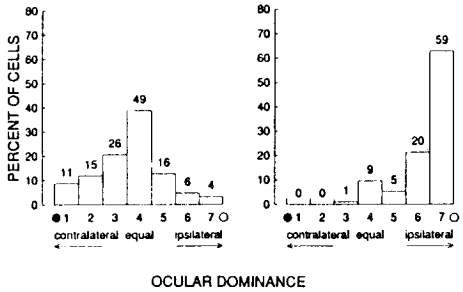

Figure 8: Ocular dominance histograms from visually responsive single units in visual cortex of 38-day old kittens, after 1 week of monocular deprivation during cortical infusion of TTX (left, 4 animals) or of vehicle solution (right, 3 animals). Conventions for histograms as in figure 7. Black dot indicates closed eye, white dot indicates open eye. Left, results from a cortical region in which all neuronal activity was blocked by cortical infusion of TTX throughout the period of monocular deprivation. Ocular dominance distribution was completely normal (compare left of figure 7), including the normal slight bias in favor of the contralateral eye, although the contralateral eye was the visually deprived eye in these animals. Right, results from a cortical region in which vehicle solution was infused throughout the period of deprivation. Most units were dominated by the open, ipsilateral eye. Data replotted from experiments reported in Reiter, Waitzman, and Stryker, 1986.

shift in ocular dominance. As expected, and consistent with the predictions of a Hebb-synapse model, the cortical activity blockade completely prevented plasticity, as is shown from the comparison of figures 7 (left) and 8.

A second assumption implicit in the Hebb-synapse explanation of development is that the statistics of neural activity are sufficient to account for ocular dominance plasticity. In nearly all of the experiments above, animals received visual experience. One might maintain that behaviorally significant visual stimulation, acting via some high-level perceptual mechanism, is crucial to plasticity in this system. In support of this notion, there is considerable evidence that behavioral state and diffuse neuromodulatory systems can influence

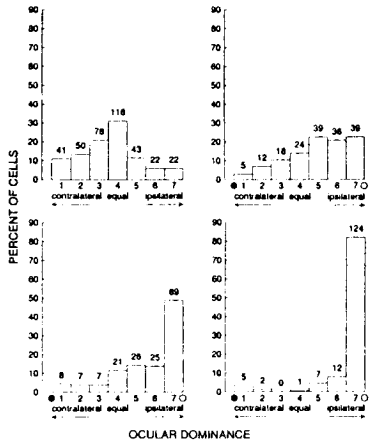

Figure 9: Ocular dominance histograms from visually responsive single units in the visual cortex of normal kittens (upper right) and of kittens subject to three different regimes by which the contralateral eye had decreased activity compared to the ipsilateral eye. Conventions for histograms as in figure 7. Black dot indicates relatively deprived eye, white dot indicates relatively more active eye. Upper left: results from six normal kittens, 36-51 days of age. Upper right: results from five kittens, 37-44 days of age, in which all retinal activity in the contralateral eye was blocked by injection of TTX, while the ipsilateral eye remained in total darkness. Lower left: results from six kittens, 36-40 days of age, in which all retinal activity in the contralateral eye was blocked by injection of TTX, and the ipsilateral eye was lid sutured. Lower right: results from four kittens, 29-34 days of age, subject to normal monocular deprivation by lid suture of the contralateral eye. Ocular dominance plasticity, resulting in a bias in favor of the ipsilateral eye, is seen in all deprivation regimes, although that at upper right and lower left included no behaviorally meaningful visual stimulation. Data replotted from experiments reported in Chapman et al., 1986.

plasticity in the visual system. These findings have led to Singer's "gating hypothesis" that plasticity occurs only when some combination of adrenergic, cholinergic, or glutamatergic "gates" are opened in visual cortex by the activity of various diffuse projection systems (Singer, 1985). To test this assumption, we attempted to produce ocular dominance plasticity in a situation in which neither eye received behaviorally significant visual stimulation (Chapman et al., 1986). Activity in one eye was blocked with TTX, while maintained but not visual activity was present in the other eye, which either remained in total darkness or received diffuse-light stimulation.

The maintained activity of the occluded eye, without any meaningful visual input, was sufficient to cause ocular dominance plasticity, as shown in figure 9. We conclude that at least much of the plasticity that takes place in the development of ocular dominance columns does not require meaningful visual input, so that it is reasonable to attempt

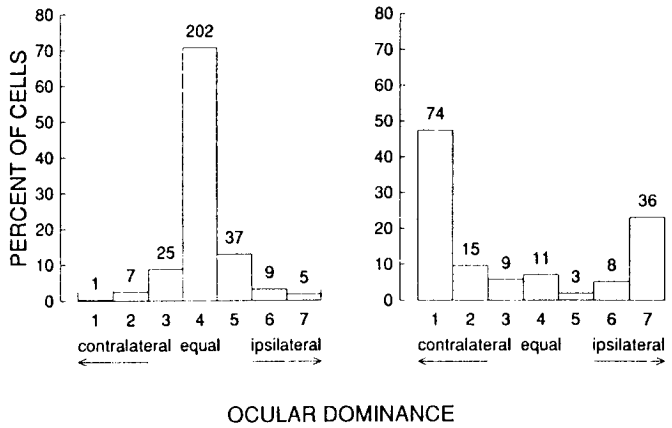

Figure 10: Ocular dominance histograms from visually responsive single units in the visual cortex of kittens after a period in which all retinal activity was blocked by injection of TTX, and the optic nerves were stimulated electrically. Conventions for histograms as in figure 7. Left: results from kittens in which the two optic nerves were stimulated simultaneously. Note that most neurons were binocularly driven. Right: results from kittens in which each optic nerve received the same pattern of stimulation as in the kittens in the left figure, but in which the relative timing of the pattern between the two eyes was such that the two eyes were stimulated alternately rather than simultaneously. Note that most neurons were driven monocularly. Unpublished data from experiments described in Stryker, 1986.

to understand its dependence on the statistics of neural discharge, as our model does.

A third assumption of the Hebb-synapse model of ocular

dominance column development is that ocular dominance segregation is governed by the relative timing of neural activity, the greater correlation in the patterns of neural discharge within each eyes' afferents than between the afferents of the two eyes. This assumption is only weakly supported by experiments showing that complete retinal activity blockade prevents ocular dominance column formation (Stryker and Harris, 1986). It is supported more strongly, but still indirectly, by the experiments showing that ocular dominance columns form more rapidly and more nearly completely when animals are reared with experimental strabismus. A direct test of the role of correlated activity was carried out by eliminating the natural maintained retinal discharge and introducing controlled patterns of activity into the two optic nerves by electrical stimulation (Stryker, 1986). These experiments showed that ocular dominance columns did not form when the the two optic nerves were stimulated simultaneously, but that an equal amount of activity delivered alternately to the two nerves did allow ocular dominance segregation. Figure 10 shows that most neurons were binocularly driven in the former case but monocularly driven in the latter.

A final assumption of the Hebb-synapse model is that not only are patterns of activity in the synaptic inputs important, but so are the responses of postsynaptic cortical cells. In numerous earlier experiments in which the responses of cortical cells were perturbed by substances infused into the cortex, ocular dominance plasticity was disrupted to a greater or lesser extent, but the presynaptic effects of these substances on afferent terminals were not known. We tested this assumption by infusing into visual cortex muscimol, a substance that powerfully inhibited cortical cells but appeared (and is thought to have) no effect on activation of or synaptic release from afferent terminals (Reiter and Stryker, 1988). In the region of cortex in which cortical discharge was completely inhibited, inputs from the less-active, occluded eye came to dominate over those from the more active, non-deprived eye, as shown in figure 11. This is a form of synaptic plasticity in the reverse direction from normal, but it is exactly what would be predicted by the Hebb-synapse model. In this

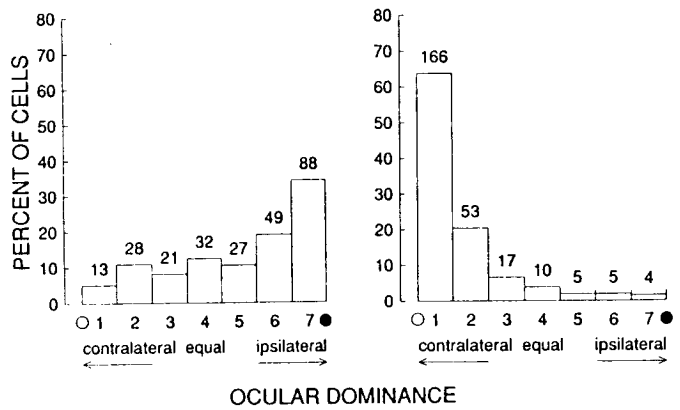

Figure 11: Ocular dominance histograms from visually responsive single units in the visual cortex of 8 kittens, 35-43 days of age, after 5-7 days of monocular deprivation during cortical infusion of muscimol. Left, results from regions in which all cortical cell neuronal activity was blocked by muscimol infusion. Right, results from the same kittens in cortical regions outside the muscimol-induced blocked. Conventions for histograms as in figure 7. Black dot indicates closed eye, white dot indicates open eye. In the muscimol-treated region (left), the less active, closed eye came to dominate cortical cell responses. In untreated regions, the normal domination by the more active, open eye was seen. Data replotted from experiments reported in Reiter and Stryker, 1988.

case, the activity of the less-active, occluded eye is better correlated with that of the inhibited postsynaptic cortical cells than is the activity of the more-active open eye. This finding confirmed the crucial role of the postsynaptic cells, as postulated in the Hebb model. Furthermore, it suggested that a process coupled to postsynaptic membrane voltage or conductance controls the direction of synaptic plasticity, which favors more-active inputs when the postsynaptic cell can be depolarized by them but less-active inputs when the postsynaptic cell is inhibited. Finally, it demonstrates that, at least for this form of plasticity, postsynaptic discharge is not essential, since the reverse plasticity took place while spikes were blocked in the cortical cells.

These experiments reveal a minimal set of features that must be incorporated in a model of ocular dominance column development in mammalian visual cortex. First, the afferents in such a model should

initially make widespread overlapping connections, some of which become ineffective or are removed in development. Second, the correlation of activity among afferents serving one eye, and the lack of correlation between the eyes, clearly plays a role. Third, postsynaptic activity in the cortex is also crucial, and, therefore, intracortical synaptic connections by which cortical cells influence one another's activity will play a role.

The model described below incorporates these three features, together with a Hebbian or other rule to govern changes in synaptic strength. These features may all be measured accurately by feasible experiments; in fact, measurements in the literature allow us to make estimates of the values of the parameters describing each. Thus, a model incorporating these features may make genuine predictions about normal development and the outcomes of experiments.

A Model of Ocular Dominance Segregation

We have developed a simple model of the segregation of geniculocortical afferents into ocular dominance columns (Miller, Keller, and Stryker, 1986, 1989). This model summarizes the properties of the initial geniculocortical anatomy and physiology and of proposed plasticity rules in three functions that describe the three features just discussed:

- An arbor function, telling the strength of the initial connection – the number of synapses – between an afferent and a cortical cell, as a function of the retinotopic distance between their receptive field centers;
- A set of afferent correlation functions, summarizing the correlations in firing between afferents as a function of the distance between their receptive field centers and of their eyes of origin;
- A cortical interaction function, telling the influence that two simultaneously active synapses have upon one another's growth, as a function of the distance between them across cortex.

This model can be used to analyze a number of proposed mechanisms of synaptic plasticity, including a Hebbian mechanism. The features that distinguish one proposed mechanism from another will be found in the different forms given by each mechanism to the three functions that summarize the initial anatomy and physiology and the plasticity rule: afferent correlations, arbor/retinotopy, and cortical interactions.

The cortical interaction function is particularly dependent upon the proposed biological mechanism of plasticity. In the case of a Hebbian synapse mechanism, the growth of a synapse is promoted if it is active simultaneously with its postsynaptic cell. A synapse, by being active, increases the chance that its postsynaptic cell will be simultaneously active. Consider two simultaneously active synapses onto two cortical cells. If the two cortical cells excite one another, then the two simultaneously active synapses tend to aid one another's growth by increasing the probability of simultaneous excitation of one another's cortical cell. If the two cortical cells inhibit one another, the two synapses tend to suppress one another's growth. Hence for a Hebb synapse, the cortical interaction function, which describes the influence of two simultaneously active synapses upon one another's growth, is determined by the spread of intracortical synaptic influences. For a mechanism involving release of a diffusible modification factor, the function involves the lateral spread of influences by diffusion as well.

A number of simplifying assumptions are embodied in this model. We assume that, in some averaged sense, it makes sense to talk about afferent correlations and about geniculocortical and corticocortical connectivity as simple functions of the distance between two cells. Afferents actually comprise several classes: on- and off-center cells, and X and Y or parvo and magno cells. Afferent correlations and arbor sizes depend upon the type of afferent. The cortex has many attributes besides position: a cortical location in layer 4 may have associated with it a specificity for orientation or other properties, and there are a variety of cortical cell types. Geniculocortical and corticocortical connections are likely to have specificity with respect to these attributes, even in the young animal before ocular dominance segregation occurs (Lund, 1988; Martin, 1988). By ignoring these details, we reduce the system to the elements that seem essential to columnar development. We similarly assume

that every synapse from a given afferent to a given cortical location experiences and exerts identical influences, ignoring neuronal microstructure. We also assume that the process controlling synaptic plasticity can be well approximated by instantaneous interactions rather than by following the detailed temporal structure of neuronal activations. We hypothesize that the tendency of two inputs to have correlated activity on a time scale determined by the plasticity mechanism is the key feature to be abstracted, and that the finer details of activity patterns can be ignored[1]. It is also assumed that the time scale associated with the activity-dependent mechanism is much smaller than the time scale over which synapses are appreciably changing their strengths; this allows averaging of the equations over all afferent activity patterns. Finally, the three functions are considered static during the initial development of a pattern of ocular dominance segregation. This simplification is potentially most problematic for the cortical interaction function, since if cortical interactions are themselves changing by an activity-dependent mechanism, their development would be coupled to the development of the geniculocortical projection.

The model need not depend on other features that might be thought critical. The measure of post-synaptic activity for purposes of plasticity may be action potentials or, as suggested by a number of recent studies (Katz and Constantine-Paton, 1988; Reiter and Stryker, 1988), local membrane depolarization. In principle, it is not even critical that the post-synaptic activity be involved at all. What is critical is that modification depend upon paired activities, either paired presynaptic activities or paired pre- and post-synaptic activities (the latter can be reduced to paired presynaptic activities via an equation like equation 4 below).

---

1. The time within which inputs must be correlated in order to influence one another's growth appears to be on the order of 10^{-1} second (Altmann et al., 1987; Blasdel and Pettigrew, 1979; see also references re LTP in hippocampus: Gustafsson et al., 1987; Larson and Lynch, 1986; Rose and Dunwiddie, 1986) while membrane times and interspike correlation times are of order 10^{-2} or 10^{-3} seconds.

Biological Characterization of the Three Functions Measurements made in cats allow estimation of the three functions that characterize the cortex in the model. As shown in figure 5, Y-cell afferents in visual cortex of young kittens appear to be capable of arborizing over an area more than 2 mm in diameter, or 1 mm in radius. This result, based on the study of putative afferents (LeVay and Stryker, 1979), is consistent with the final extent of patchy Y-cell arborizations seen in adults (Humphrey et al., 1985a,b). X-cell afferents have not been filled in kittens before columns develop, but based on the extent of patchy arborizations in adults (Humphrey et al., 1985a,b), it appears that X-cells might initially arborize over a region 0.5–0.75 mm in radius.

The ocular dominance patches of adult cats have a periodicity of about 850 μm (width of right-eye plus left-eye patches) (Anderson, Olavarria, and Van Sluyters, 1988; LeVay, Stryker, and Shatz, 1978; Shatz, Lindstrom, and Wiesel, 1977; Swindale, 1988). This period appears to be smaller than, or perhaps about the same size as, the diameter of initial X-cell afferent arborizations and seems clearly smaller than the diameter of initial Y-cell afferent arborizations.

Measurements of maintained activity of retinal ganglion cells in darkness in adult cats demonstrate that nearby ganglion cells have correlated activities, due to their common inputs (Mastronarde, 1983a,b). No indications of anticorrelations at further distances were seen[2]. Converting the retinotopic distance between correlated ganglion cells to a retinotopic distance across cortex (Tusa, Palmer, and Rosenquist, 1978), it appears that incoming afferents representing a single eye are correlated across cortical distances of from 1/2 (X-cells) to 3/2 (Y-cells) of a geniculocortical arbor radius. As previously noted, there may also be more widespread correlations within each eye on longer time scales (Levick and Williams, 1964; Rodieck and Smith, 1966). These estimates are very crude, as they are based upon

2. ON-cells are correlated with ON-cells, and OFF-cells with OFF cells. ON-cells are anticorrelated with OFF-cells over similar distances; no indication of correlation with increasing distance is seen in this case. Some possible implications of the anticorrelations between ON and OFF cells are briefly discussed later in this chapter.

measurements in the retina rather than the LGN and in adults rather than kittens. Further measurements are needed.

Horizontal intracortical synaptic interactions are the feature in the model that is least well characterized experimentally. In adult cat, these connections are likely to be excitatory at short range, and appear to be inhibitory to distances of perhaps 400-500 μm (Hata, et al., 1988; Hess, Negishi and Creutzfeldt, 1975; Toyama, Kimura, and Tanaka, 1981a,b; Worgotter and Eysel, 1989). Long-range synaptic interactions exist over distances of 1 mm or more (Gilbert and Wiesel, 1983). These long-range interactions connect only discrete patches of cortex and so may quantitatively have less impact than the shorter-range interactions. In the adult, the long-range connections may connect cells of similar orientation specificity by excitatory connections, and may also make inhibitory contributions to direction-selectivity (Tso, Gilbert, and Wiesel, 1986; Worgotter and Eysel, 1989). In the kitten, even before patch development but after the development of orientation selectivity, the long-range connections appear to connect patches with a periodicity consistent with that of orientation columns, as well as with that of the subsequent ocular dominance columns (Luhmann, Martinez Millan and Singer, 1986).

In summary, knowledge of the three functions involved in the model is still rudimentary, but better measurements can and will be made. In the adult, incoming afferents from a single eye appear correlated over 1/2–3/2 of an afferent arbor radius, while anticorrelations between more distant inputs thus far have not been seen. The ocular dominance patches themselves appear to have a period less than, or perhaps equal to, an afferent arbor diameter. Intracortical synaptic interactions appear to be excitatory at short distances and inhibitory at greater horizontal distances in the adult, over distances that are within an arbor radius. In addition, there may be longer range connections with a definite periodicity. We will return to these points after examination of the model and its behavior.

In general, the model and its behavior will first be described intuitively, with a minimum of mathematics. Then more mathematical detail may be presented, keyed by a section heading or lead sentence referring to "mathematical" results. The reader with little mathematical interest may wish to skim or skip these sections; results in other sections do not depend upon them.

General Formulation of the Model We model the cortex as a 2-dimensional lamina, representing layer 4, and the LGN as two 2-dimensional laminae, one representing each eye. Let Roman letters such as x designate a 2-dimensional position on the cortex, and Greek letters such as α designate a 2-dimensional retinotopic position in the LGN. We assume retinotopic location can be directly interconverted with cortical location, via the retinotopic map onto cortex[3].

Let $S^L(x,\alpha,t)$, $S^R(x,\alpha,t)$ represent total synaptic strength at time t of the afferents of left or right eye, respectively, from $\alpha \rightarrow x$. Since an afferent may make many synapses onto a cortical cell, S may represent a sum of strength over many synapses. The number of such synapses is defined by the arbor function, $A(x-\alpha)$. Let $s_j^L(x,\alpha,t)$ represent the strength of the j^{th} individual synapse of the left-eye from α to x. Then S^L is defined by $S^L(x,\alpha,t) \equiv \sum_{j=1}^{A(x-\alpha)} s_j^L(x,\alpha,t)$. We take A to be a single static function for all cells, while s and S vary in time.

The afferent correlation and cortical interaction functions are defined as follows (figure 12). The correlation functions $C^{LL}(\alpha-\beta)$ and $C^{LR}(\alpha-\beta)$ describe the correlation in firing between the left-eye afferent with retinotopic position α, and the left- or right-eye afferent, respectively, with retinotopic position β. $C^{RL}(\alpha-\beta)$ and $C^{RR}(\alpha-\beta)$ are defined similarly. The cortical interaction function $I(x-y)$ describes the influence of simultaneously active synapses at x and y upon one another's growth.

Our model equation for cortical synaptic plasticity is

$$\frac{dS^L(x,\alpha,t)}{dt} = \lambda A(x-\alpha) \sum_{y,\beta} I(x-y)[C^{LL}(\alpha-\beta)S^L(y,\beta,t) + C^{LR}(\alpha-\beta)S^R(y,\beta,t)] - DECAY^L(x,\alpha,t) \quad (1)$$

3. The retinotopic map onto cortex is linear in a local region of cortex. We assume it to be isotropic, ignoring differences in magnification with direction across cortex or LGN. Hence it is assumed to be a simple identity map between the cortical and geniculate grids.

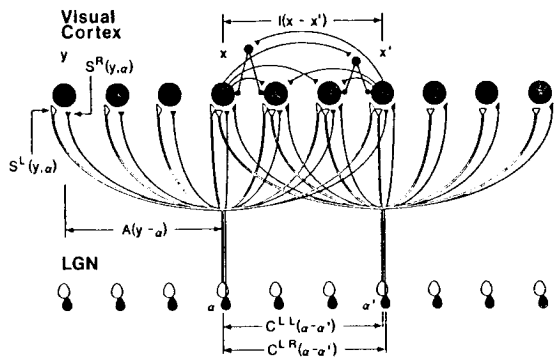

Figure 12: Notation. Afferents from left-eye (white) and right-eye (black) layers of the LGN innervate layer 4 of the visual cortex. The LGN is modeled as consisting of two layers, one serving each eye. Each layer is two-dimensional, though only one dimension is illustrated. The cortex is modeled as a single, two-dimensional layer. In the figure, α and α' label two-dimensional positions in the LGN, and x and x' label the retinotopically corresponding points in the cortex; y labels an additional position in the cortex. The afferent correlation functions C^{LL} (correlation in activity between two left-eye afferents) and C^{LR} (correlation in activity between a left-eye and a right-eye afferent) are functions of separation across the LGN. The arbor function A measures anatomical connectivity (number of synapses) from a geniculate point to a cortical point, as a function of the retinotopic distance between them. The cortical interaction function I depends on a distance across cortex. The left-eye and right-eye synaptic strengths, S^L and S^R, from a geniculate location to a cortical location, depend upon both locations. S^L and S^R change during development in the model, while the arbor function A is held fixed; the assumption is made that anatomical changes occur late in development, after a pattern of physiological synaptic strengths is established. From Miller, Keller, And Stryker, 1989. Copyright 1989 by the AAAS.

where $DECAY^L(x,\alpha,t) = \gamma S^L(x,\alpha,t) + \varepsilon A(x-\alpha)$ for some constants γ and ε. The equation for S^R is identical with interchange of L and R everywhere. The DECAY term involves changes in each synapse independent of all other synapses, while the non-DECAY term describes changes due to interactions between synapses.

The synaptic interaction term can be expressed in words as follows. First, the change in time of any synapse's strength is a sum of the influences exerted on it by all other synapses, so that the equation is linear in the variables s and thus in S. Second, the influence of any one synapse upon another is a product of the correlation between their activities, which gives a measure of the

likelihood that the two synapses fire together; the strength of the influencing synapse, which tells the amount of influence exerted by that synapse when it is active; and the strength of the intracortical interaction between them, which tells the attenuation or change in sign with cortical distance of the influence exerted. Third, the change in the total synaptic strength S between an afferent and a cortical cell is given by multiplying the total influence on one such synapse by the number of synapses from the afferent to the cortical cell. That number is given by the arbor function. This multiplication occurs because each such synapse receives identical influences.

In studying this equation we will ignore boundary effects. Stripe width is at least an order of magnitude smaller than the overall width of striate cortex. We assume that the three functions C,A, and I are relatively local, and hence most stripes develop without any direct influence of the boundaries. Thus, the boundaries should not influence the occurrence and width of periodic segregation, and it is on these features that our analysis will focus. The boundaries may influence the overall form or layout of the stripes, which we will not attempt to analyze[4]. Thus, we do away with the boundaries, either by using periodic boundary conditions (in simulations) or by assuming an infinitely wide cortex.

Equation 1 for S^L and the corresponding equation for S^R constitute our basic mathematical model of synaptic strength development. The data used in the model are the arbor function $A(x-\alpha)$, the cortical interaction function $I(x-y)$, and the correlation functions such as $C^{LL}(\alpha-\beta)$. When the initial values of S^L and S^R are given at time t=0, the equations determine S^L and S^R at any later time t.

Geniculocortical synapses are exclusively excitatory. Furthermore, synapses are limited in strength. Therefore, this basic model must be modified to prevent synaptic strength from becoming negative or from becoming too large. Nonlinearities must be included

4. The occurrence and width of segregation are determined by simple linear interactions, as will be described, and hence are robust features determined by very general features of a model. In contrast, the overall form of the pattern is determined by nonlinear interactions.

in the equation to enforce these conditions.

In addition, the total synaptic strength supported by a cortical cell or afferent may be limited beyond the extent implicit in the limits on the strengths of individual synapses. There is no direct evidence for such limits, but the phenomena associated with ocular dominance plasticity are suggestive of a competition for finite resources between afferents serving the two eyes. Such limits may also be suggested by biological evidence for limits to the total number of synapses supported by a cell. In the goldfish optic tectum, if presynaptic cells are forced to innervate only half of a normal tectum, the number of synapses formed per postsynaptic cell remains the same as in the normal case, so that on average each input forms only half its normal number of synapses (Hayes and Meyer, 1988b; Murray, Sharma, and Edwards, 1982). This suggests that the presynaptic inputs may be competing for a fixed number of postsynaptic sites. Similarly, if only a fraction of the normal presynaptic cells are allowed to innervate the tectum, the number of synapses formed per postsynaptic cell is smaller than in the normal case, suggesting intrinsic limits to the number of synapses that each presynaptic cell can make (Hayes and Mayer, 1988a). Presynaptic limits have also been observed in other systems (Fladby and Jansen, 1987; Brown, Jansen and Van Essen, 1976; Schneider, 1973). We refer to such limits as *constraints* on the total synaptic strength supported by a postsynaptic or presynaptic cell. The use of such constraints in modeling was first suggested by von der Malsburg (1973). To test the possible role of constraints in development, the model can be modified to limit the total synaptic strength supported by a cortical or afferent cell. Terms must be added to the equations to enforce such limits.

Mathematical Derivation of the Model Equation From a Hebbian Mechanism Equation 1 can be simply derived from a linear Hebb synapse mechanism. The Hebb synapse rule can be expressed, for individual synapses, as

$$\frac{ds_j^L(x,\alpha,t)}{dt} = \lambda[POST(x)PRE^L(\alpha)] - decay \qquad (2a)$$

where POST(x) is some function of postsynaptic activity at x, $PRE^L(\alpha)$

is some function of presynaptic activity from α in the left eye, and λ is a constant. Let $c(x,t)$ be the activity of the cortical cell at position x at time t, and similarly let $a^L(\alpha,t), a^R(\alpha,t)$ represent the activity of left- and right-eye afferents. Taking post to be a linear function of c (see the Appendix for the nonlinear case), this is

$$\frac{ds_j^L(x,\alpha,t)}{dt} = \lambda[c(x,t) - c_1]f_1[a^L(\alpha,t)] - \gamma s_j^L(x,\alpha,t) - \varepsilon' \qquad (2b)$$

where c_1 is a constant, f_1 is a function that may incorporate threshold or saturation effects, and γ and ε' are intrinsic decay (or growth) factors. Summing over j on both sides, this can be reexpressed as

$$\frac{dS^L(x,\alpha,t)}{dt} = \lambda A(x-\alpha)[c(x,t) - c_1]f_1[a^L(\alpha,t)] - \gamma S^L(x,\alpha,t) - \varepsilon' A(x-\alpha) \qquad (3)$$

The cortical activities in this equation can be replaced by a function of afferent activities and synaptic strengths. Define the net geniculate input to a cortical cell by

$$NET_{LGN}(x) \equiv \sum_\alpha \left\{ S^L(x,\alpha,t) f_2[a^L(\alpha,t)] + S^R(x,\alpha,t) f_2[a^R(\alpha,t)] \right\}$$

f_2 incorporates thresholds and saturations, like f_1 in equation 2. If cortical activity is a linear function of NET_{LGN} (again, the nonlinear case is considered in the Appendix), then

$$c(x,t) = \sum_y I(x-y) NET_{LGN}(y) + c_2. \qquad (4)$$

$I(x-y)$ describes the total influence on cortical point x of geniculate excitation of the cortical point at y, including direct excitation (when $y=x$), as well as indirect effects via intracortical synaptic connections by which the activity[5] of the cortical cell at y influences activity at x.

c_2 represents intrinsic activity of cortical cells in the absence of geniculate input. Substituting equation 4 for $c(x,t)$ into equation 3, and averaging over input activity patterns[6], we obtain the model equation, equation 1. Let $< >$ denote the average. Then[7]

$$C^{LL}(\alpha-\beta) \equiv < f_1[a^L(\alpha,t)] f_2[a^L(\beta,t)] >, \quad C^{LR}(\alpha-\beta) \equiv < f_1[a^L(\alpha,t)] f_2[a^R(\beta,t)] >$$

and

$$\varepsilon \equiv \varepsilon' - \lambda[c_2 - c_1] < f_1[a^L(\alpha,t)] >$$

Which Mechanisms Can Be Studied Within This Framework? We have shown elsewhere (Miller, Keller, and Stryker, 1989) that equation 1 may be derived from a number of proposed biological plasticity mechanisms. These include mechanisms involving activity-dependent release by either cortical cells or afferents of a diffusible modification factor, combined with activity-dependent

---

5. The nature of I can be further understood if we postulate, instead of eq 4, $c(x,t) = NET_{LGN}(x) + \sum_y B(x-y)c(y,t) + c'$ where $B(x-y)$ summarizes the effects of cortico-cortical synaptic interconnections, and c' is intrinsic activity of the cortical cell in the absence of all input. Assume that cortical activity is determined by afferent activity, so that the matrix $(\mathbf{1}-\mathbf{B})$ is invertible (where $\mathbf{1}$ is the identity matrix). Then equation 4 follows, with, as matrix equations, $\mathbf{I} = (\mathbf{1}-\mathbf{B})^{-1} = \mathbf{1} + \mathbf{B} + \mathbf{B}^2 + \cdots$ and $\mathbf{c_2} = \mathbf{I}c'$.

6. We have continued to use the notation S for $<S>$ after averaging. Averaging produces an infinite series of terms, of which we keep only the first. Higher order terms involve the tendency of three or more afferents to be active conjointly beyond the extent predicted by pairwise correlations. These terms are small either for small fluctuations or for small $\lambda, \gamma, \varepsilon$. Averaging is done by the smoothing procedure, described in Keller (1977) and in Miller (1989c).

7. As $\alpha - \beta \to \infty$, $C^{IJ} \to (\alpha-\beta) < f_1[a^I(\alpha,t)] > < f_2[a^J(\beta,t)] >$. Hence if $< f_1[a] > \neq 0$ and $< f_2[a] > \neq 0$, the various C's converge to a constant at large distances. This constant is the constant $-k_2$ of Linsker (1986a-c). Because it disappears from C^D and hence from the equation for S^D, described later in this chapter, it has no influence on the initial development of ocular dominance segregation.

of chemospecific adhesion such that retinotopically matched afferents and cortical cells adhere best to one another.

The mechanisms that lead to equation 1 have three points in common. They all include some arboreal and/or retinotopic factor $A(x-\alpha)$, and some lateral interconnection, either synaptic or via chemical diffusion or transport, between points in cortex. They also depend for modification upon paired activity which, via equation 4, reduces to dependence on paired afferent activities. The mathematical model common to these mechanisms, excluding the decay terms, can be summed up by the following heuristic for the interactions between synapses:

$$\frac{dS^L(x,\alpha,t)}{dt} = \sum_{E=L,R}\sum_{y,\beta}[\text{Influence Felt by } S^L(x,\alpha,t)][\text{Influence Exerted by } S^E(y,\beta,t)]$$

Here the influence felt by $S^L(x,\alpha,t)$ is $f_2[a^L(\alpha,t)]A(x-\alpha)$, that is, some measure of the presynaptic activity of the synapse, multiplied by the number of synapses from α innervating x (perhaps scaled by the retinotopic affinity of synapses from α for x). The influence exerted by $S^E(y,\beta,t)$ is $f_1[a^E(\beta,t)]S^E(y,\beta,t)I(x-y)$, that is, some measure of the presynaptic activity of these synapses, multiplied by the total synaptic strength of such synapses, times a factor indicating the influence felt at a distance across cortex from the influencing synapse.

The mechanisms have one additional point in common. Synapses causing modification act in proportion to their total strength, S^L or S^R, while synapses being modified respond independently of their strength, but in proportion to their total number A. Biologically, the first feature seems natural, but the second is arbitrary given our current biological knowledge. Choosing to let synapses exert influence in proportion to A results in a trivial theory. With this choice, synaptic strengths do not interact. Instead, all synapses simply decay or grow uniformly. Thus, the only interesting alternative choice is to let both influence exerted and influence felt be proportional to S. In this case, the lowest-order term embracing synaptic interactions is intrinsically nonlinear. However, in certain limits this case, also,

approaches equations like those we study[8].

Because several different biologically reasonable mechanisms of synaptic plasticity are described by the same mathematical formalism, agreement between the predictions from a particular mechanism and the biological reality can not by itself be taken as strong evidence in favor of the mechanism. Such agreement appears at first sight only to distinguish among very large classes of mechanisms, where the members of a class make similar predictions. Therefore, one is led to question the extent to which such models can be informative to biologists. It is important to note, however, that different mechanisms are distinguished by the different biological features that are summarized in the three functions characterizing the mathematical model. That is, these functions will have different biological interpretations under different mechanisms. Furthermore, as we will show, measurements of these functions can allow prediction of whether ocular dominance segregation should occur, and the

8. Let $S^S = S^L + S^R$, $S^D = S^L - S^R$. Assume equivalence of the two eyes, and ignore decay. Then for this case, before averaging over input activity patterns,

$$\frac{dS^D(x,\alpha,t)}{dt} = \tfrac{1}{2}S^S(x,\alpha,t)\sum_{y,\beta} I(x-y)\,C^D(\alpha-\beta,t)\,S^D(y,\beta,t) \qquad \text{(N1)}$$

$$+\tfrac{1}{2}S^D(x,\alpha,t)\sum_{y,\beta} I(x-y)\,C^S(\alpha-\beta,t)\,S^S(y,\beta,t)$$

Here,

$$C^S(\alpha-\beta,t) = f_1[a^L(\alpha,t)]\left\{f_2[a^L(\beta,t)] + f_2[a^R(\beta,t)]\right\},$$

$$C^D(\alpha-\beta,t) = f_1[a^L(\alpha,t)]\left\{f_2[a^L(\beta,t)] - f_2[a^R(\beta,t)]\right\}.$$

Note that $\langle C^S\rangle = C^{LL} + C^{LR}$, $\langle C^D\rangle = C^{LL} - C^{LR}$. Suppose there are constraints on the sum S^S such that receptive fields are relatively uniform across the cortex, except for ocular dominance. Then $S^S(x,\alpha,t) \approx f(x-\alpha,t)$ for some function f. Suppose that S^S and S^D can be taken to be statistically independent. Then, after averaging, the first term in equation N1 becomes the non-decay term in equation 5, with f playing the role of an arbor function. The second term in equation N1 contributes to the decay term in equation 5.

periodicity of such segregation if it does occur. Therefore, experimental measurements of the biological features that define the functions under the assumption that one or another mechanism is active, can serve to distinguish among the mechanisms of synaptic plasticity.

Studying the Model Through Simulations

Simulations of Development and Deprivation We have studied the behavior of the model through computer simulation of development, by carrying equation 1 forward in time from an initial state in which synapses of the two eyes have nearly equal strengths. For this purpose, we model cortex and the left- and right-eye layers of the LGN as three 25×25 layers of neurons. To eliminate boundary effects, we use periodic boundary conditions, so that the leftmost and rightmost columns of each grid are adjacent, as are the bottom and top rows. Each geniculate cell is connected to a 7×7 square of cortical cells, centered about the retinotopically corresponding cell in the cortical grid.

Initially, we consider the following choice of functions. The arbor function is equal to 1 over the 7 x 7 set of connections and 0 outside. The correlation function includes positive correlation within each eye, falling to zero over about an arbor radius; there is neither correlation nor anticorrelation between the eyes ("same-eye correlations", gaussian parameter 0.3, in figure 13).

The cortical interaction function is excitatory among nearest neighbors on the grid, and weakly inhibitory more peripherally for several gridpoints (Mexican hat cortical interaction in figure 13). Other choices of functions will be examined subsequently. Each of the 2×7×7×25×25=61,250 synapses is assigned an initial weight randomly drawn from a distribution uniform between 0.8 and 1.2. Synaptic weights grow or decay according to the model equation until they reach 8.0 or 0, at which point no further change is allowed.

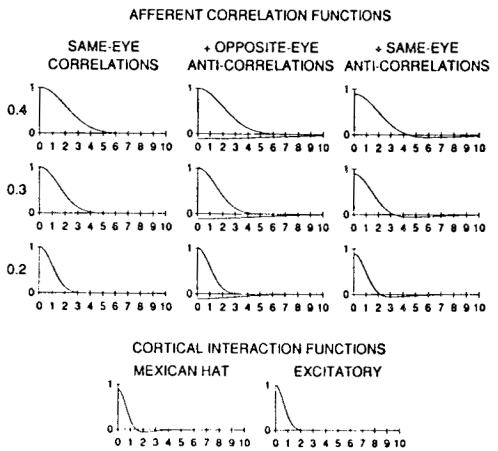

Figure 13: Functions used for simulations of full geniculocortical innervation. Function value, vertical axis, versus distance in grid intervals, horizontal axis. All functions are circularly symmetric in two dimensions. **Top**: Correlation functions $C(\alpha)$. These summarize the correlation in activity between two afferents separated by the retinotopic distance α. We assume $C^{LL}(\alpha)=C^{RR}(\alpha)$, $C^{LR}(\alpha)=C^{RL}(\alpha)$. The correlation functions in the left column (same-eye correlations) are positive within each eye, and zero between the two eyes: $C^{LL}(\alpha)=e^{-\alpha^2/(\kappa D)^2}$, where $D=7$ is the arbor diameter and $\kappa=0.4$, 0.3 or 0.2 for the top, middle, or bottom row respectively, and $C^{LR}=0$. The positive correlations within each eye are shown. The correlation functions in the middle column (+ opposite-eye anticorrelations) are positive within each eye as in the left column, as shown by the curves above the horizontal axes; but in addition there are weaker, more broadly ranging negative correlations between the two eyes, shown by the curves below the horizontal axes. These negative correlations are given by $C^{LR}(\alpha)=-1/9e^{-\alpha^2/(3\kappa D)^2}$. The correlation functions in the right row (+ same-eye anticorrelations) have these same negative correlations added to the positive correlations within each eye, and have zero correlation between the two eyes. This creates a "Mexican hat" function within each eye, so that inputs are correlated at shorter distances and anticorrelated at longer distances, as illustrated. **Bottom**: Cortical interaction functions I(x). Left, Mexican hat function, given by gaussians as for the rightmost correlation functions but with $\kappa=0.1333$. Right, a purely excitatory cortical interaction function, given by the excitatory gaussian of the Mexican hat function. From Miller, 1989a.

Constraints are added, fixing the total synaptic strength on a cortical cell and fixing or limiting the total synaptic strength coming from each afferent. We will subsequently discuss the effect of these constraints.

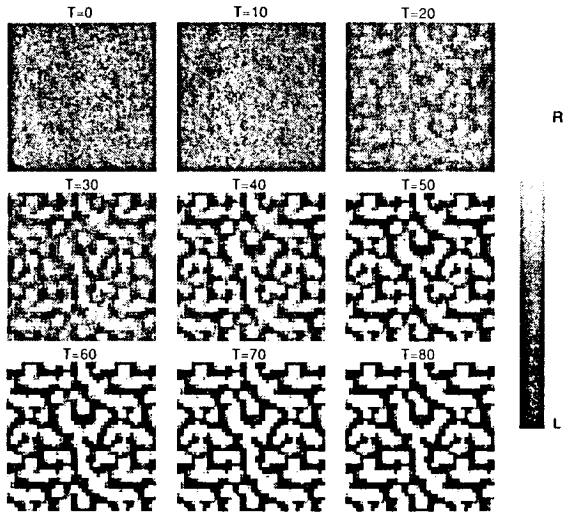

Figure 14: Development of ocular dominance of cortex in the model. Cortex is shown at nine times, from time 0 to the 80th iteration. Each pixel represents a single cortical cell. The greyscale represents ocular dominance D of each cell, the difference between the total strength of right-eye and of left-eye geniculate inputs to the cell: $D(x) \equiv \sum_{\alpha}[S^R(x,\alpha)-S^L(x,\alpha)]$. The greyscale runs linearly from monocular for the right eye (white) to monocular for the left eye (black). Final (timestep 200) cortex is the lower right of figure 15. This development used the following functions (figure 13): The correlation functions have same-eye correlations only, with parameter 0.3. The intracortical interaction function is Mexican hat. The arbor function is taken to be 1 over a 7×7 arbor, 0 elsewhere. Constraints were used to conserve total synaptic strength over each cortical cell and over each afferent arbor (Miller, 1989c; Miller, Keller, and Stryker, 1989). *Convention for all simulations*: Illustrations of cortex show 40×40 grids, although the model cortex is 25×25. Periodic boundary conditions were used, so this display shows continuity of the pattern across what would otherwise appear to be a boundary. Thus, the top 15 and bottom 15 rows within each square are identical, as are the left 15 and right 15 columns. From Miller, 1989c.

The randomly assigned synaptic strengths result in an initially nearly uniform innervation by the two eyes, much like that seen by autoradiography in the young kitten before segregation of left-eye from right-eye afferents. Segregation and development of an overall pattern of ocular dominance in the model cortex occurs even while the

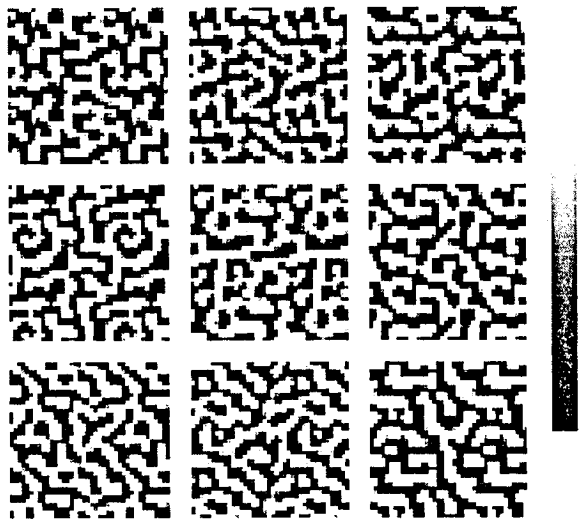

Figure 15: Cortex, timestep 200, resulting from nine different random initial conditions. Cortical interaction, arbor, and correlation functions and conventions as in figure 14. Results are qualititatively and quantitatively similar for all initial conditions that have been tried; that is, the 2-dimensional Fourier transforms yield similar power spectra. From Miller, 1989c.

amplitude of the pattern is still quite small, perhaps smaller than could be detected experimentally. This is illustrated in figure 14. In this figure, each pixel represents the ocular dominance of a single cortical cell. Black or white represent dominance by left or right eyes, respectively, while intermediate greys represents equality or varying degrees of dominance of the two eyes. The pattern continues to develop as it grows nearly to saturation, so that most cortical cells eventually become fully monocular, completely dominated by one eye or the other. The resulting development and final pattern of ocular dominance closely resembles the patterns of periodic segregation seen in cat or monkey, although cat layer 4 has more binocular cells than this model cortex. This development is completely robust across randomly generated initial conditions: every initial condition leads, given this same choice of functions, to a qualitatively similar, though distinct, final outcome. Figure 15 illustrates the final cortices resulting from nine different sets of initial synaptic strengths.

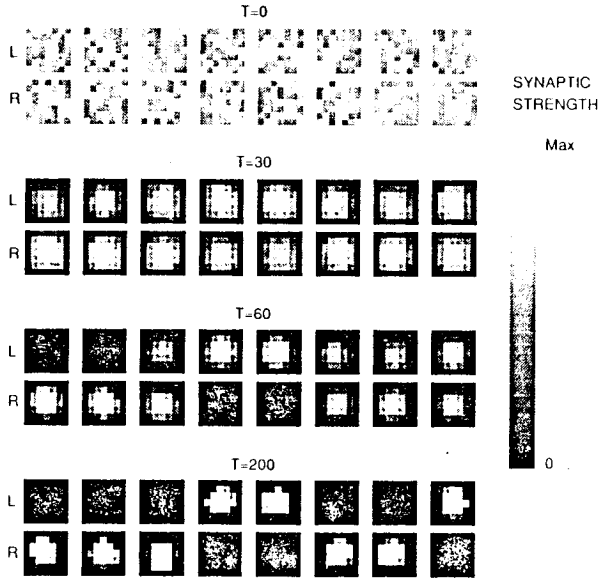

Figure 16: Receptive fields (ignoring the contribution of corticocortical connections) of eight cortical cells at timesteps 0, 30, 60, 200. Each vertical L,R pair of large squares shows strengths of the 7×7 left-eye and 7×7 right-eye synapses onto a cortical cell at one time. Synaptic strengths onto eight adjacent cortical cells are shown. Cortical cells shown are the eight leftmost cells in the bottom row of the cortices of figure 14. The greyscale varies linearly in synaptic strength from 0 (black) to the maximum strength present at the given timestep (white). These maximum strengths are: timestep 0, 1.2; timestep 30, 3.3; timesteps 60 and 200, 8.0. Receptive fields first refine in size, concentrating their strength centrally. They then become monocular with synaptic strength confined to left- or right-eye inputs. Adjacent groups of cells tend to become dominated by the same eye, providing the basis for ocular dominance segregation across the cortex as a whole. From Miller, 1989c.

The pictures of cortex just presented collapse information about the 98 synapses onto each cortical cell into a single pixel representing net ocular dominance. More can be learned by examining in detail the development of each individual synapse onto a given cortical cell. The geniculate synapses onto the cortical cell represent the cell's receptive field, discounting the effects of cortico-cortical synaptic connections. We illustrate (figure 16) the development of these receptive fields for 8 cortical cells. These are the 8 leftmost cortical

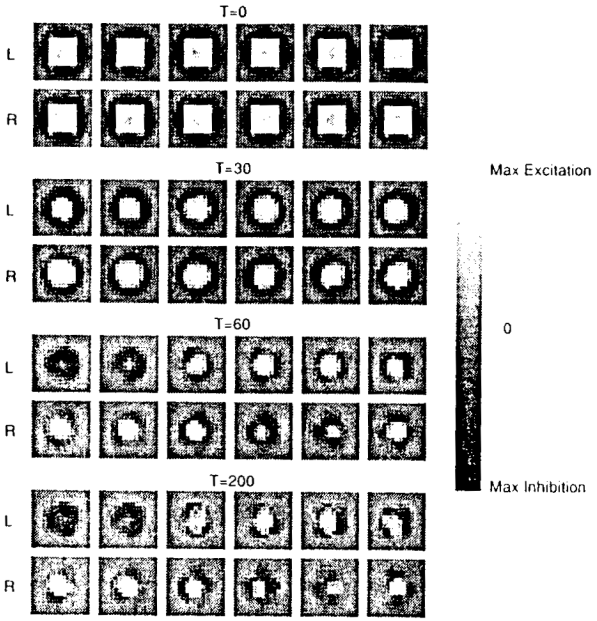

Figure 17: Physiological receptive fields at timesteps 0, 30, 60, 200, for the six leftmost cortical cells of the 8 shown in figure 16. Each vertical L,R pair shows physiological input to the cortical cell from 15×15 left-eye or right-eye geniculate positions. Physiological input from a geniculate cell is defined as the linear sum of the cell's direct synaptic input onto the cortical cell, and its synaptic input onto other cortical cells weighted by the synaptic influence of those cortical cells on the cortical cell observed. Thus, physiological input to a cortical cell at x from the left-eye geniculate position α is defined by $P^L(x,\alpha) = \sum_y I(x-y)S^L(y,\alpha)$. Input may be excitatory (grey, strength 0, to white, maximum excitatory strength present at a timestep) or inhibitory (grey, strength 0, to black, maximum inhibitory strength present at a timestep). Maximum excitatory strengths at the four times, respectively, are 1.4, 4.1, 13.6, 14.4; maximum inhibitory strengths are -0.6, -0.9, -2.5, -2.9. At time 0, the 7×7 arbor of direct synaptic connections provides excitatory input, while surrounding geniculate positions give inhibition. Development of physiological receptive fields parallels the development of the direct geniculocortical input shown in figure 16, but in addition the development of sidebands of inhibitory input from the dominant eye and of inhibitory input from the nondominant eye can be observed. From Miller, 1989c.

cells in the bottom row of the cortices of figure 14. Each vertical pair of 7×7 "L" and "R" squares displays the strengths of the 49 left-eye and 49 right-eye synapses onto one cortical cell at one developmental time. The receptive fields first refine in size, while developing only weak biases of ocular dominance. Subsequently, the receptive fields become monocular as they continue to refine in size.

Intracortical synaptic interconnections modify cortical receptive fields. Assuming local excitation and more distant inhibition between cortical cells as given by the excitatory/inhibitory cortical interaction function, and using a simple linear model of cortical activation[9], we can compute the resulting receptive fields. This is illustrated in figure 17, for the six leftmost cells of the eight illustrated in figure 16. Two features are added to cortical receptive fields by intracortical connectivity. First, the nondominant eye gains input to the cortical cell, but it is inhibitory input, as occurs physiologically in some cases (Bishop, Henry, and Smith, 1971; Kato, Bishop, and Orban, 1981; Ohzawa and Freeman, 1986). Second, though the receptive fields initially develop a circularly symmetric structure as they refine, this circular symmetry of individual receptive fields is broken as each eye's inputs become segregated into its eye-specific stripes. While this is reminiscent of the development of orientation selectivity in cortical cells, it cannot explain that phenomenon, because orientation selectivity develops biologically even in regions of cortex where there is innervation by only a single eye.

Just as we can study the receptive fields of individual cortical cells, we can study the terminal arbors – the projection onto cortex – of individual geniculate afferents. These arbors are illustrated in the same format used for the receptive fields in the absence of intracortical connectivity (figure 18). Vertical pairs of "L" and "R"

9. Our crude, linear model of cortical activation can be sufficient to study the periodic segregation of ocular dominance, as we will discuss, but it lacks the detail to make precise predictions about the effects of intracortical synapses on physiological receptive field structure. Thus, results with this linear model are only intended to be suggestive of some of the additional features that intracortical connectivity might add to receptive fields; results might be altered considerably by nonlinearities.

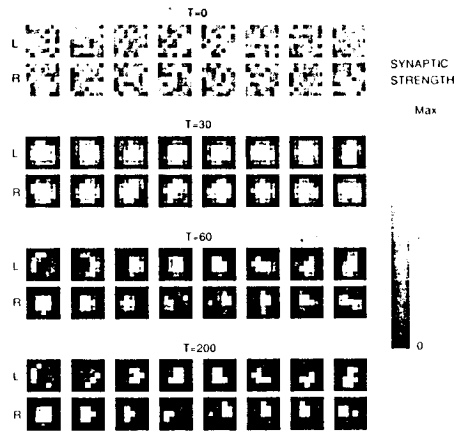

Figure 18: Afferent arbors at timesteps 0, 30, 60, 200. Conventions as in figure 16, except that here the strengths of the synaptic arbors projected by eight adjacent left-eye and eight adjacent right-eye LGN afferents onto cortex are pictured, whereas in figure 16 the strengths of the left-eye and right-eye synapses received by 8 cortical cells were pictured. The afferents shown are the eight leftmost cells in the bottom row of the respective geniculate grids. Thus, each vertical L, R pair illustrates the arbors of a left- and a right-eye geniculate cell from identical geniculate grid positions at one time. Greyscale shows synaptic strength of connection to each of the 7 by 7 cortical cells contacted by the arbor. Arbors first concentrate their strength centrally, then break up into patches confined to complementary cortical ocular dominance patches. From Miller, 1989c.

7×7 squares here display the strengths of the synapses projected to cortex by the left-eye and right-eye afferents representing a single receptive field location. The arbors initially refine in size much like the receptive fields, but then segregate into complementary cortical regions as each eye's input becomes confined to the appropriate eye's patches. This is reminiscent of the terminal arbors in the cat (figure 5). Thus, many features of normal biological development emerge in the model. These include periodic ocular dominance segregation across cortex, refinement and development of monocularity in individual cortical receptive fields, and refinement and confinement to patches of afferent arbors.

Using the same choice of functions and the same initial conditions as in the simulation just presented, we now proceed to study the effects of visual deprivation.

Monocular visual deprivation is modelled as a decrease in the amount of activity within one eye, and hence, as a decrease in the amplitude of the correlation function within that eye. Possible disruption of the correlational structure within the deprived eye, which would only increase the effects of deprivation, is ignored. We consider the effects on the final cortex of initiating monocular deprivation at increasingly later times in development (figure 19). With early initiation of deprivation, the "open" eye takes over much

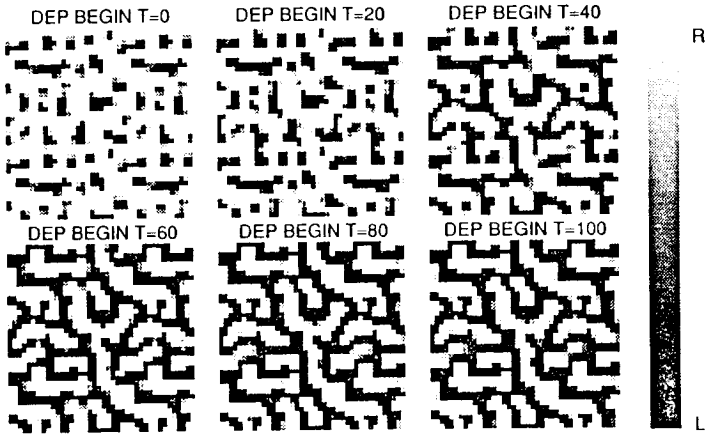

Figure 19: Cortical patterns of ocular dominance resulting from sustained monocular deprivation initiated at various times. Results of initiating the deprivation at iteration 0, 20, 40, 60, 80, or 100 are shown. All parameters, functions, and initial conditions are identical to those used in figure 14, except that (1) the deprived eye's correlation function was multiplied by 0.7 during the deprivation, and (2) Only partial constraints on afferent arbors were used, so that afferent arbors were able to vary their total synaptic strength by ±50 percent from the original value. Final cortices (T=200) are shown for each case. Synaptic strengths were frozen upon reaching the limiting values of 0 or 8; this makes very little difference in final results for these functions (Miller, 1989c). From Miller, 1989c.

more than its normal share of cortex. As in biological development, there is a critical period for this phenomenon in the model: the later in development deprivation is initiated, the less effect deprivation has, and with sufficiently late initiation there is no effect. The precise degree of ocular dominance shift produced by deprivation initiated at

a particular time in development depends upon model parameters. These include the amount by which activity in the deprived eye is reduced and the degree of change allowed in the total synaptic strength supported by an afferent arbor[10]. It is very robust, however, that early onset of deprivation leads to strong ocular dominance shifts, and that initiation of deprivation progressively later in development leads to progressively smaller effects.

This critical period occurs in the model for two reasons. First, there is a strictly dynamical or organizational component. As ocular dominance segregation proceeds, each eye attains dominance in synaptic strength within its stripes. Since the influence of synapses involves a product of the presynaptic activity times the synaptic strength, this dominance in synaptic strength can more than compensate for the decrease in activity caused by deprivation and allow the deprived eye to maintain dominance within its stripes. Second, there is a component due to "stabilization" of synapses: once synapses are fully saturated (strength 8.0 or 0), they may be frozen, so that they are no longer allowed to change in strength. If stabilization of synapses is used, no changes in ocular dominance can occur once most synapses have been saturated.

With correlation functions like that used here, or more broadly ranging, layer 4 normally becomes fully monocular (as will be discussed). Then dynamical or organizational factors are sufficient to entirely account for a critical period. In this case, the critical period is unchanged by the presence or absence of stabilization: it emerges entirely from the fact that a sufficient degree of ocular dominance organization becomes dynamically irreversible. When correlation functions are narrower, the final layer 4 normally includes a greater

10. In the simulation shown, we have used constraints allowing progressively less change in the total synaptic strength over an afferent arbor as that total approaches ±50 percent of its initial value. Afferents are not allowed to gain or lose more than 50 percent of their total strength, although they continue to redistribute strength between their synapses even after the 50 percent limit is reached. Deprivation initiated at time 0 leads deprived-eye arbors to shrink to the maximum degree allowable, and to disappear completely if that is allowed. Later initiation of deprivation leads to smaller effects, irrespective of the precise constraint used.

number of binocular cells. Such an outcome may also result if the development of vision tends to correlate the activity of the two eyes and if these changes occur while segregation is incomplete. Binocular cells remain dynamically susceptible to an ocular dominance shift at any stage of development. Hence, if the final layer 4 includes a significant percentage of binocular cells, as in the cat, a complete explanation of a critical period requires stabilization of saturated synapses. In this case, however, dynamical factors will still contribute to the critical period by ensuring that regions sufficiently dominated by one eye will no longer be subject to an ocular dominance shift. The biological critical period may, of course, involve other factors such as molecular changes that switch off the possibility of plasticity, in addition to the factors discussed here.

Functional Dependence of the Simulation Results The results above resulted from simulation using a particular choice of the correlation, cortical interaction, and arbor functions. The shapes of these functions are not well known in developing animals and, furthermore, it will be of experimental interest in the future to perturb these functions to study the effect upon development. Hence, to connect the model to biology, the dependence of developmental results on the choice of the correlation, cortical interaction, and arbor functions must be understood.

To determine this dependence, we have systematically varied each function. In the results that follow, one function at a time is varied, while the other two functions are left identical to those used in the simulation illustrated in figs. 16 and 18-20. The random initial conditions in all cases are identical to those used for that simulation, to facilitate comparison of results. This does not allow a complete exploration of the parameter space, but in combination with our analytical results, discussed subsequently, yields an understanding of the role played by each function in ocular dominance segregation.

We first consider the effects of varying the correlation functions. Figure 13 illustrates a series of correlation functions obtained by broadening or narrowing a gaussian correlation function within each eye ("same-eye correlations"). To such gaussian correlations within each eye, weak, more broadly ranging gaussian anticorrelations may be added either between the two eyes ("+ opposite-eye anticorrelations"), or within each eye ("+ same-eye anticorrelations").

Opposite-eye anticorrelations can be considered a model of strabismus or of alternating monocular deprivation; but such anticorrelations might also be present during normal development as a result of inhibitory interactions within the LGN. Same-eye anticorrelations are of interest both because of their use in other models (Linsker, Chapter 10), and because it is possible that they too might be introduced in the LGN or by the statistics of retinal response to visual input.

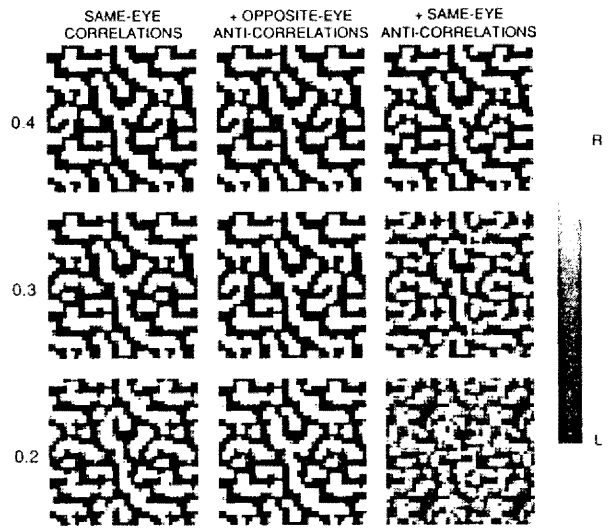

Figure 20: Development of ocular dominance using the nine afferent correlation functions illustrated in figure 13. Initial conditions, conventions, and all functions (cortical interaction, arbor) save the correlation function are as in figure 14. Cortex is shown in its final state (timestep 200). Broader correlations, or opposite-eye anticorrelations, lead to increased monocularity of the final cortex without changing the basic periodicity. Same-eye anticorrelations lead to decreased monocularity. If present within an arbor radius (0.2), same-eye anticorrelations lead to a largely binocular cortex with a weak and irregular pattern of ocular dominance segregation. The periodicity of this pattern is fundamentally altered from the others and is quite noisy (distributed over many wavelengths).

Results of simulations using each of these correlation functions are shown in figure 20. Broader correlations within each eye or addition of opposite-eye anticorrelations leads to a more completely

monocular cortex. This agrees with experimental findings in which artificially induced strabismus or alternating monocular deprivation, which induce anticorrelations or reduce correlations between the eyes, lead to an increase in monocularity throughout the cortex (Hubel and Wiesel 1965). Narrower correlations within each eye lead to more binocular cells at the borders between eye stripes without otherwise altering the pattern of stripes. Same-eye anticorrelations also lead to more binocular cells at the borders between eye stripes and, if significant within an arbor radius ("same-eye anticorrelations 0.2"), tend to destroy monocularity and to destroy the regular cortical organization of ocular dominance. In this case, afferents from a single eye giving input to different halves of a single cortical cell's receptive field are anticorrelated with one another. Then development of one eye's strength in one part of the cell's receptive field discourages development of that same eye's strength elsewhere in the same field, leading to binocularity.

The above results on narrowing of the correlation function suggest that even nearest neighbor correlations might be sufficient to yield ocular dominance segregation. To test this, a gaussian correlation function within each eye ("same-eye correlations 0.4") was set equal to zero outside squares of various sizes (Miller, 1989C). Correlation only between afferents within one square ring of one another[11] is sufficient to yield monocular cells and a normal periodic pattern of segregation. Correlation over an arbor radius (3 square rings) seems both necessary and sufficient to yield a completely monocular layer 4. Similar conclusions result from the study of correlation functions that are constant over some distance, and equal to zero outside (Miller, 1989C)[12]. An increase in the amplitude of the correlations can largely, but not completely, compensate for a decrease in spatial extent. In all of these cases, when segregation occurs, it appears to occur with an invariant period.

Next, we consider the effects of varying the cortical interaction

11. α and β are within N square rings of each other if $|\alpha_1-\beta_1|\leq N$ and $|\alpha_2-\beta_2|\leq N$.

12. The correlation functions used were $C(0)=1$; $C(\alpha-\beta)=c$ for $\alpha\neq\beta$, α and β within N square rings of one another; $C(\alpha-\beta)=0$ otherwise.

function. Results using a purely excitatory cortical interaction function, without the more peripheral inhibition present in the Mexican hat function studied previously (figure 13), depend critically on the presence of constraints conserving the sum of synaptic strength over an afferent arbor. In contrast, results obtained with the Mexican hat function depended little on such constraints. Figure 21 shows the

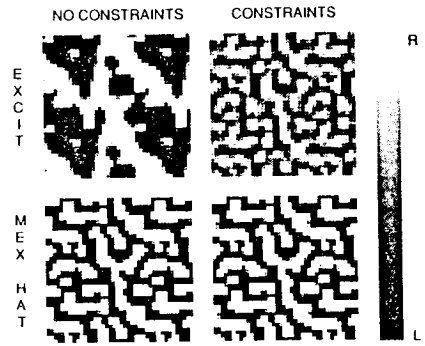

Figure 21: Cortical patterns of ocular dominance resulting from development with the excitatory cortical interaction function of figure 13, with and without constraints fixing the total synaptic strength over each afferent arbor. For comparison, results using the Mexican hat cortical interaction function of figure 13, with identical constraints, are shown below. The final cortex (T=200) is shown in each case. Functions, initial conditions, and conventions otherwise as in figure 14. Constraints on the total synaptic strength over a cortical cell are as in figure 14; only the constraint on total strength over an afferent is being varied. In the absence of constraints, the excitatory function leads to an arbitrarily large scale of ocular dominance segregation; constraints lead to segregation with width of left-eye plus right-eye stripes equal to about an arbor diameter. Much greater monocularity of segregation is seen if a slightly broader correlation function ("same-eye correlations 0.4") is used (Miller, 1989a; Miller, Keller, and Stryker, 1989). The Mexican hat function selects a width of segregation smaller than an arbor diameter, and results are unaffected by the constraints. From Miller, 1989c.

periodic pattern of ocular dominance resulting from the purely excitatory cortical interaction function, and from the Mexican hat cortical interaction function, in the presence or absence of such constraints. In the absence of constraints, a purely excitatory cortical interaction leads one eye to take over large regions of cortex, while the opposite eye loses all input to these regions. Constraints force

afferents to redistribute strength, rather than to uniformly gain or lose strength, and thus force the two eyes to retain equal cortical innervation. This leads a periodic pattern of ocular dominance segregation to develop even when the cortical interaction function is entirely excitatory. Close examination reveals that the average width of the periodicity in this case is somewhat greater than with the Mexican hat cortical interaction function. The width of right-eye plus left-eye bands is now about an arbor diameter, as will be explained

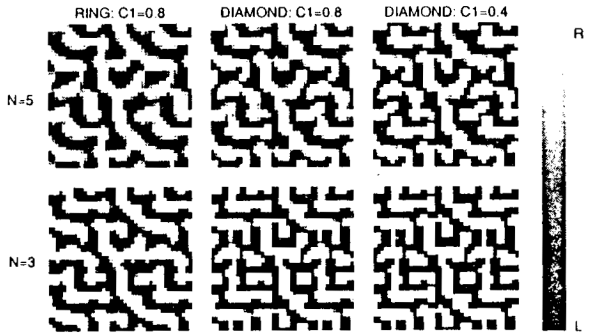

Figure 22: Cortices resulting from development with varying cortical interaction functions. These functions were zero outside of N=5 or 3 square rings. Functions were equal to c_1 (0.8 or 0.4) over either one square ring ("RING") or over the diamond of four nearest neighbors on the grid ("DIAMOND"), and equal to a constant negative value elsewhere, adjusted so that the function sums to zero. The correlation function used was "same-eye correlations 0.4". Arbor function and initial conditions as in figure 14. Cortices shown at T=100; runs were only carried out to that time. From Miller, 1989c.

below.

We have studied a variety of other forms of mixed excitatory/inhibitory cortical interaction functions. The resulting cortices, shown in figure 22, illustrate that the same initial conditions can lead to broader or narrower ocular dominance patches as the intracortical interactions are varied.

Finally, the effect of using an arbor function that tapers over the 7 x 7 region in which the arbor function is nonzero has been studied. Normal periodic segregation occurs, but if there are constraints fixing the total synaptic strength over an arbor, then the width of the

periodicity is decreased (Miller, 1989c). The effect is like that of using a smaller arbor.

To summarize, the model robustly reproduces periodic ocular dominance segregation like that seen experimentally, beginning from an essentially uniform initial innervation by the two eyes. Individual cortical receptive fields refine in size and grow monocular; physiological fields develop inhibition from the nondominant eye. Afferent arbors refine in size and restrict their innervation to the appropriate eye's patches. The effects of monocular deprivation are reproduced, and a critical period is seen. Broader correlations within each eye, or anticorrelations between the eyes as in strabismus, enhance monocularity, while narrower correlations or anti-correlations within an eye reduce monocularity. Changes in the correlation function do not obviously modify the width of periodic segregation, provided that segregation occurs. A purely excitatory cortical interaction function is sufficient to yield ocular dominance patches, provided arbors are constrained to conserve their total synaptic strength. The width of the periodic pattern can be altered by varying the cortical interaction or arbor functions.

We now seek to understand more generally what is responsible for periodic segregation. Can we predict the forms of the correlation, cortical interaction, and arbor function that will lead to segregation, and can we predict the width of the stripes that will result when segregation does occur?

Analysis of the Model

To analyze the model, we assume equality of the two eyes (ignoring the case of monocular deprivation, and relatively small asymmetries in normal development). This means $C^{LL} = C^{RR} = C^{SameEye}$, $C^{LR} = C^{RL} = C^{OppEye}$. We analyze the development of the *difference* between the two eyes' synaptic strengths, $S^D(x,\alpha,t) \equiv S^L(x,\alpha,t) - S^R(x,\alpha,t)$. The equation for S^D is

$$\frac{dS^D(x,\alpha,t)}{dt} = \lambda A(x-\alpha)\sum_{y,\beta} I(x-y)C^D(\alpha-\beta)S^D(y,\beta,t) - \gamma S^D(x,\alpha) \qquad (5)$$

where $C^D(\alpha-\beta) \equiv C^{SameEye}(\alpha-\beta) - C^{OppEye}(\alpha-\beta)$. C^D represents the degree to which an afferent is more correlated with another afferent from its own eye than with an afferent from the opposite eye, at a fixed retinotopic separation.

Initially the innervations representing the two eyes are nearly equal. Hence S^D is very nearly zero everywhere. If this difference were initially exactly zero everywhere, it would stay so forever. Each eye's synapses would experience exactly the same environment at each moment in time, and we have assumed that the two eyes obey identical rules. Given the small perturbation in the difference, however, one can imagine two outcomes: either the small perturbation might decay to a state of complete equality; or it might grow, developing into some large pattern of differences between the two eyes. We will analyze whether the condition of equality is stable to small perturbations. If it is unstable, we will determine the pattern that will grow out of the instability.

This analysis, as to the existence and nature of a possible pattern-forming instability, depends only upon the behavior of the model very near the condition of complete equality. In this region, S^D is very small, hence nonlinear terms are negligibly small. Therefore, only the linear terms in S^D play a role in this region. Thus, even quite complicated, nonlinear models can be reduced, near the condition of equality, to a linear equation. If the linear equation we use for S^D approximates the linear equation resulting from a nonlinear model, our results will describe the pattern formation expected in such a fully nonlinear model.

To conduct this analysis, we determine the patterns of ocular dominance that grow or decay exponentially and independently, each at its own rate, in the linear regime. We call these the characteristic patterns of ocular dominance. Each choice of functions yields a distinct set of characteristic patterns and growth rates. If some of the patterns have a positive growth rate for a given choice of functions, so that they will grow in time rather than decay, then the condition of equality will be unstable to small perturbations for that choice of functions. In this case, we determine the characteristic patterns of ocular dominance that grow most quickly. These patterns are spatially periodic. Their wavelength determines the *width* of the final periodic pattern of ocular dominance across cortex that will result for that choice of functions. This is the width of a complete cycle of right-eye plus left-eye ocular dominance patches or stripes. This width is determined by the wavelengths of the fastest-growing patterns, because in the linear regime these patterns quickly dominate. The *form* that this periodic pattern takes – blobs, patches, stripes, hexagons – depends on the nonlinearities, and cannot be predicted from such a simple analysis.

This discussion can be expressed mathematically. Write equation 5 as $\frac{dS^D(x,\alpha,t)}{dt} = LS^D(x,\alpha,t)$ where L stands for the linear operator on the right side of equation 5. Suppose we can find eigenfunctions of the operator L, that is, a set of functions $S_i^D(x,\alpha)$ such that $LS_i^D(x,\alpha) = \omega_i S_i^D(x,\alpha)$ for constants ω_i, where i is an index enumerating the eigenfunctions. The constants ω_i are the *eigenvalues* of the operator L. Suppose further that these eigenfunctions are *complete* in the sense that any initial condition $S_0^D(x,\alpha) \equiv S^D(x,\alpha,t=0)$ can be expressed as a linear sum of these eigenfunctions: $S_0^D(x,\alpha) = \sum_i c_i S_i^D(x,\alpha)$ for some constants c_i[13]. Then the solution to equation 5 is $S^D(x,\alpha,t) = \sum_i c_i e^{\omega_i t} S_i^D(x,\alpha)$. If the real equation has nonlinearities, this solution only holds near the initial condition, where the c_i are small and the equation remains effectively linear.

From this mathematical solution we can conclude several things about development of S^D near the initial condition. First, in this region the eigenfunctions each grow independently of one another, with the rate of growth of each determined by its eigenvalue ω_i. The eigenfunctions are thus the characteristic patterns of ocular dominance, defined above; while the eigenvalues (or, in the case of complex eigenvalues, the real parts of the eigenvalues) are the growth rates of the characteristic patterns. Second, if any of the growth rates are positive, the corresponding characteristic patterns will grow rather than decay from the initial condition (this assumes that, in the perturbation representing the initial condition, none of the c_i are exactly zero). Hence, the condition for a pattern-forming instability is

13. If $I(x)=I(-x)$ and $C^D(x)=C^D(-x)$, the substitution $S'^D(x,\alpha,t) = \frac{S^D(x,\alpha,t)}{\sqrt{A(x-\alpha)}}$ transforms L into a symmetric operator; hence in this case L will have a complete set of eigenfunctions, with real eigenvalues.

the presence of at least one positive growth rate. Third, if there is such an instability, the exponential growth in time of each pattern ensures that the fastest growing patterns will quickly outgrow the others and dominate the final solution. This is the basis for the statement that the fastest-growing pattern in the linear regime sets the wavelength, even in the final fully non-linear conditions.[14] If there are a variety of fastest-growing patterns, for example, ones involving parallel ocular dominance stripes of a fixed wavelength but each with stripes oriented in a different direction across cortex, then the final form of the overall pattern will depend on the initial conditions and upon dynamical interactions among these individual oriented patterns. Such interactions are exclusively nonlinear; hence, the form but not the wavelength of the final pattern is determined by the nonlinearities in the process.

The Characteristic Patterns of Ocular Dominance

The characteristic patterns of ocular dominance are the patterns of S^D that grow independently and exponentially, each at its own rate, from an initial condition of near equality of the two eyes. Each characteristic pattern of ocular dominance consists of a characteristic receptive field of ocular dominance, and an oscillation of ocular dominance across cortex. Figure 23 shows the fastest growing such pattern for the functions used in the simulation of figure 14. The characteristic receptive field is the pattern of differences between left- and right-eye synaptic strengths in the input to a cortical cell. Where it is positive one eye is dominant, and where it is negative the opposite

14. It is possible for the initial pattern that develops out of an instability to be only metastable, so that eventually it may reorganize into a pattern with a different period determined by nonlinearities. This seems unlikely in the ocular dominance system, as studies of development of ocular dominance columns (LeVay, Stryker, and Shatz, 1978) show no obvious change in periodicity between its earliest detection and the final adult pattern. With the use of voltage sensitive dyes (Blasdel and Salama, 1986), it may be possible to test this by following development of the columns within a single animal.

eye is dominant. A monocular characteristic receptive field, like that of figure 23, is one dominated by a single eye throughout, so that the

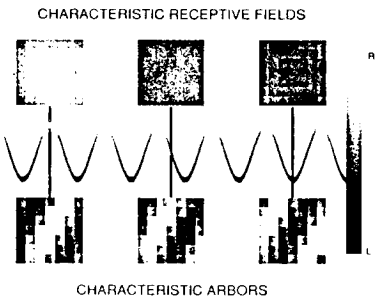

Figure 23: A monocular characteristic pattern of ocular dominance. The characteristic receptive field, and associated characteristic arbor, are illustrated at three cortical locations. The sinusoid illustrates the oscillation of ocular dominance across cortex associated with the characteristic pattern, correctly scaled to the arbor and receptive field sizes. Greyscale codes S^D, the difference between the synaptic strengths of the two eyes, varying from dominance by one eye to dominance by the other. The pattern shown here is one of the set (identical except for rotations of the direction of the oscillation) of fastest-growing characteristic patterns for functions used in the simulation of figure 14. The characteristic receptive field illustrates the retinotopic positions from which a cortical cell at a given position in cortex receives stronger left-eye or right-eye geniculate input. The characteristic arbor illustrates the cortical positions to which the left eye or right eye geniculate afferents representing a given retinotopic position project more strongly. At the cortical point corresponding to the leftmost receptive field, cortical cell inputs are dominated by the right eye everywhere within the receptive field. Afferents with the corresponding retinotopic position therefore project arbors such that the right eye afferents preferentially project to the central patch of the arbor (cortical right-eye stripe) and the left-eye afferents preferentially project to the peripheral patches in the cortex (cortical left-eye stripe). Similarly, the central receptive field is at the border between left-eye and right-eye stripes, where the two eyes have equal innervation, and the rightmost receptive field is in the center of a left-eye stripe. The oscillation projects in a direction perpendicular to the stripes across the arbors, rather than horizontally as depicted.

characteristic receptive field can be taken positive everywhere. Characteristic receptive fields need not be monocular: they may be binocular, showing division of the receptive field into domains dominated by opposite eyes. The characteristic receptive field will be positive in the domains dominated by one eye, and negative in the domains dominated by the opposite eye.

The characteristic receptive field represents the pattern of ocular dominance *within* a cortical receptive field. The characteristic pattern of ocular dominance also includes an oscillation in the degree of dominance of receptive fields across the cortex. This is an oscillation of ocular dominance *between* receptive fields across the cortex. In figure 23, the leftmost receptive field occurs at a cortical point where the right eye is dominant. The central receptive field occurs at a point that differs by 1/4 cycle of the cortical oscillation, so the two eyes are equal. The rightmost receptive field occurs at a point that differs by 1/2 cycle of oscillation, so the left eye is dominant. At points a distance across the cortex corresponding to an integral number of full cycles of oscillation, the right eye is again dominant. In the case of monocular characteristic fields, it is this oscillation, between ocular dominance by one eye and by the other, that causes organization of monocular cortical cells into ocular dominance patches. We refer to the spatial period or wavelength of this oscillation as the wavelength of the characteristic pattern. This wavelength corresponds to the width of left-eye patch plus right-eye patch, which we refer to simply as the patch width.

As figure 23 indicates, the characteristic receptive fields have associated with them characteristic afferent arbors, given by multiplying the receptive field by the oscillation in ocular dominance. In other words, when characteristic receptive fields are monocular, so that ocular dominance patches arise, the afferent arbors will only innervate the patches from the relevant eye. Thus, characteristic arbors show patches with a periodicity equal to that of the cortical oscillation, as is seen both in the simulations and in actual biological development.

Different characteristic patterns, then, are distinguished by (1) The nature of their characteristic receptive field; (2) The wavelength of the oscillation of ocular dominance across cortex. The characteristic receptive field may be monocular, corresponding to development of ocular dominance segregation, or binocular, corresponding to a cortex in which every cell receives input from both eyes. If it is monocular, the wavelength of the cortical oscillation will determine the patch width of ocular dominance organization associated with the pattern. Many patterns will compete from the initial condition of near equality of the two eyes; those that grow fastest will win out. If the fastest-growing patterns are all monocular

and all have a similar wavelength, the cortex will develop ocular dominance organization with that wavelength.

To express these results mathematically, transform variables in equation 5 from cortex and LGN (x,α) to cortex and receptive field (x,r), where $r=x-\alpha$. The resulting equation is a simple convolution in the cortical variable x. By fourier transform, such a convolution has eigenfunctions of the form $S^D_{mj}(x,\alpha)=e^{im\cdot x}R_{mj}(r)$[15], where m is a two-dimensional real vector, the wavevector of cortical oscillation, and j is an additional index of the eigenfunctions for a given m. R is a characteristic receptive field, because it represents the dependence of the eigenfunction upon r for a fixed cortical position x. We can also write this as $S^D_{mj}(x,\alpha)=e^{im\cdot\alpha}B_{mj}(r)$ where $B_{mj}(r)\equiv e^{im\cdot r}R_{mj}(r)$. B represents the dependence of the eigenfunction upon r for a fixed afferent position α, and hence is a characteristic arbor.

These eigenfunctions are complex. If $I(x)=I(-x)$ and $C^D(\alpha)=C^D(-\alpha)$, the real part and imaginary part of a complex eigenfunction are both real eigenfunctions, with the same eigenvalue. These real eigenfunctions can be chosen of the form $\cos k\cdot x\, R^+(r)+\sin k\cdot x\, R^0(r)$, where R^0 has zero net ocular dominance ($\sum_r R(r)=0$) and R^+ may have net ocular dominance. For the eigenfunction illustrated in figure 23, $R^0\equiv 0$; the nonmathematical discussion was simplified by neglect of the possibility that R^0 may be nonzero[16].

---

15. We are assuming here, and subsequently, either an infinite grid or a continuum. On the finite grid with periodic boundary conditions of the simulations, we would instead obtain $e^{\frac{2\pi m\cdot x}{L}}R_{mj}(r)$ where the finite grid is of length L and m is a two-vector of integers.

16. To construct real eigenfunctions, note that, if the operator L can be made symmetric (see note 12), the complex conjugate of an eigenfunction is also an eigenfunction with identical (real) eigenvalue. Hence, given any eigenfunction S^D_{mj}, its real part S^R_{mj} and its imaginary part S^I_{mj} are both real eigenfunctions with the same eigenvalue. Let R^R and R^I be the real and imaginary parts, respectively, of R. Then these real eigenfunctions are

$$\begin{bmatrix} S^R_{mj}(x,\alpha) \\ S^I_{mj}(x,\alpha) \end{bmatrix} = \begin{bmatrix} \cos mx & -\sin mx \\ \sin mx & \cos mx \end{bmatrix} \begin{bmatrix} R^R_{mj}(r) \\ R^I_{mj}(r) \end{bmatrix}$$

Thus real eigenfunctions involve a sinusoidal mixing, across cortex, between R^R

In summary, if the fastest-growing characteristic pattern of ocular dominance is monocular – that is, if its characteristic receptive field is monocular – it will yield segregation across cortex into ocular dominance patches. The width of a cycle of these patches will be given by the wavelength of the pattern's associated cortical

---

and R^I. Note that S^R and S^I are identical except for a cortical phase shift of 90°.

A more convenient representation can be found by shifting phase so that one of the two basis receptive fields has zero dominance. The subscript [mj] will be assumed where not explicitly indicated. Define the (unnormalized) dominance of an eigenfunction by $D \equiv |\sum_r R(r)|$, and define the angle θ by $\sum_r R(r) = De^{i\theta}$. Define new complex eigenfunctions by $\tilde{S}^D = e^{-i\theta}S^D = e^{i\tilde{k}\cdot x}\tilde{R}$ where $\tilde{R} = e^{-i\theta}R$. The imaginary part of $\tilde{R}$ has zero dominance, $\sum_r \tilde{R}^I(r) = 0$, while the real part of $\tilde{R}$ has the maximum dominance for any cortical phase of receptive fields associated with that eigenfunction, $\sum_r \tilde{R}^R(r) = D$. The new real eigenfunctions are given by

$$\begin{pmatrix} \tilde{S}^R_{mj}(x,\alpha) \\ \tilde{S}^I_{mj}(x,\alpha) \end{pmatrix} = \begin{pmatrix} \cos\theta_{mj} & \sin\theta_{mj} \\ -\sin\theta_{mj} & \cos\theta_{mj} \end{pmatrix} \begin{pmatrix} S^R_{mj}(x,\alpha) \\ S^I_{mj}(x,\alpha) \end{pmatrix}$$

Define $R^+ \equiv \tilde{R}^R$, $R^0 \equiv \tilde{R}^I$. Then

$$\begin{pmatrix} \tilde{S}^R_{mj}(x,\alpha) \\ \tilde{S}^I_{mj}(x,\alpha) \end{pmatrix} = \begin{pmatrix} \cos mx & -\sin mx \\ \sin mx & \cos mx \end{pmatrix} \begin{pmatrix} R^+_{mj}(r) \\ R^0_{mj}(r) \end{pmatrix}$$

Hence the eigenfunctions can be described as a sinusoidal mixing, across cortex, between a maximum-dominance (for that eigenfunction) receptive field, and a zero-dominance receptive field. Figures 23-25 illustrate R^+ and R^0 for each eigenfunction.

In the general case, the operator L is not assumed symmetrizable. The fact that L is real ensures that $\tilde{S}^D_j$ and its complex conjugate $\tilde{S}^{D*}_j$ are both eigenfunctions, with complex conjugate eigenvalues. If the leading eigenvalues are not real, the result will be temporal oscillations of ocular dominance. These will combine with the spatial oscillations to yield traveling waves of ocular dominance. This is discussed in more detail in Miller, 1989c. One expects that such an effect should be suppressed in any reasonable theory, so that the leading eigenvalues will always be real, although empirically it is not impossible that such waves could exist early in development.

oscillation. Afferent arbors will become confined to those periodic patches. To understand the development of ocular dominance segregation within the model, then, it is sufficient to answer two questions: (1) Under what circumstances will the fastest growing pattern be monocular? (2) When it is monocular, what will determine the wavelength of its cortical oscillation?

Monocularity and Wavelength of the Fastest Growing Patterns

The results of both analysis and computation lead to the following conclusion: The fastest growing patterns are monocular whenever the correlation function C^D is positive at least between nearest neighbors, and not significantly negative within an arbor radius. In this case, the wavelength of cortical oscillation is the wavelength corresponding to the maximum of the fourier transform of the cortical interaction function.

Intuitively, this can be understood as follows. By a correlation-based mechanism, an individual cortical cell develops two features. First, its receptive field comes to consist of inputs whose activities are mutually correlated. To the extent to which, in the local area sampled by the cortical cell, this represents inputs from a single eye, the cortical cell will become monocular. Alternatively, when there are same-eye anticorrelations within an arbor radius, the most correlated inputs are obtained if one part of the receptive field represents one eye, and an adjacent part of the receptive field represents the opposite eye. This yields a binocular field. Second, due to cortical interactions, a cortical cell's receptive field becomes both maximally correlated with the receptive fields of neighboring cortical cells at distances over which the cortical interactions are excitatory, and minimally correlated (or maximally anti-correlated) with the receptive fields of neighboring cortical cells at distances over which cortical interactions are inhibitory. For a monocular cell, this is best achieved when nearby cells within the region of excitatory cortical interactions are monocular cells that represent the same eye; while more distantly neighboring cells, within the region of inhibitory cortical interaction, are monocular cells from the opposite eye. This cannot be achieved simultaneously for all cells; but it is most nearly achieved, over all cells, by matching the cortical oscillation of the ocular dominance

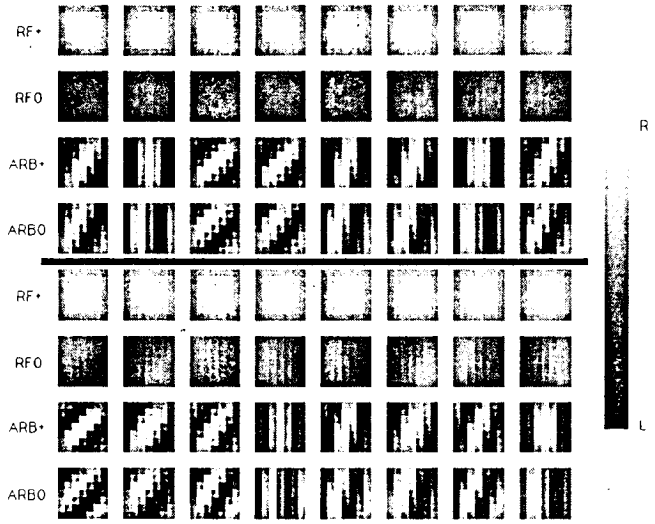

Figure 24: The 16 fastest-growing characteristic patterns of ocular dominance for the functions used in the time development of figure 14. Each vertical set of four squares shows, from top to bottom, the maximum dominance receptive field, the minimum dominance receptive field, the arbor corresponding to the maximum dominance position, and the arbor corresponding to the minimum dominance position. These correspond, respectively, to the leftmost receptive field, central receptive field, leftmost arbor, and central arbor in figure 23. The 16 patterns are arranged in decreasing order of growth rate, so that the fastest growing is at upper left and most slowly growing of the 16 at lower right. For each pattern, additional patterns with identical growthrates exist, differing only by rotations or reflection of the pictured pattern. All the leading patterns have highly monocular receptive fields. They differ significantly only in the precise width and orientation of their cortical oscillations, which is visible as the oscillation across the arbors. From Miller, 1989c.

pattern to the dominant wavelength in the cortical interaction.

We will illustrate these results both through direct computations of the characteristic patterns for varying parameters, and by analytic solutions to the equations in various limiting cases.

Computation of the Characteristic Patterns We can directly compute the characteristic patterns for the model when it is placed on a grid as in the simulations of time development. For the choice of functions used in the time development displayed in figure 14, for which C^D

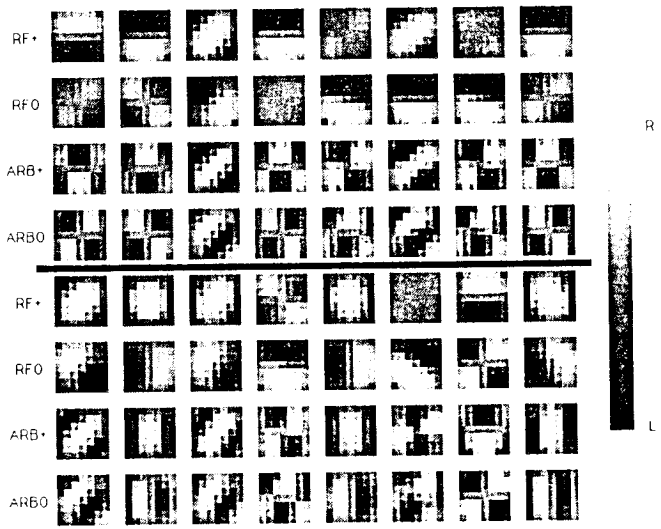

Figure 25: The sixteen fastest-growing patterns for the correlation function "+ same-eye anticorrelations 0.2", with functions otherwise as in figure 24. The fastest-growing patterns are binocular. Conventions as in figure 24. From Miller, 1989c.

satisfied the above criteria for emergence of monocularity, the fastest growing characteristic patterns are indeed monocular (figure 24). There are 625 oscillation frequencies on the 25×25 grid, and for each such frequency there are 49 characteristic patterns due to the 7×7 arbor. Among the 49 characteristic patterns with a single oscillation frequency, for the same choice of functions, only a single pattern – the fastest growing one for that frequency – is monocular (Miller, 1989c). Thus, monocular patterns are rare among all possible patterns, yet they are selected as the fastest-growing for this choice of functions. In contrast, with a different choice of correlation function that includes prominent anticorrelations within an arbor radius ("+ same-eye anticorrelations 0.2"), the fastest growing patterns across all frequencies are binocular (figure 25). For this correlation function, only weak and irregular ocular dominance segregation developed in simulations (figure 20).

Results across all frequencies and for varying correlation functions are shown in figure 26. This figure illustrates the results of computation of the characteristic patterns for each of the nine sets of

functions, identical except for varying correlation functions, whose developmental outcome was illustrated in figure 20. The graphs show the growth rate (vertical axis) of the characteristic patterns versus their inverse wavelength (horizontal axis). The graph's grey scale represents the monocularity of patterns: the shading at a point corresponds to the degree of monocularity seen for patterns with the given wavelength and growth rate, from lightest for fully monocular, to black for fully binocular. The curves show analytic predictions for the growth rates as a function of wavelength, derived in limiting cases that will be discussed. In particular, the lower thin lines show the fourier transform of the cortical interaction function, whose peak accurately predicts the wavelength of the fastest-growing patterns.

Increasing the breadth over which the correlation function C^D is positive increases the monocularity of the fastest-growing patterns and increases the dominance in growth rate of monocular patterns over binocular patterns. The breadth of C^D is increased either by broadening of within-eye correlations, or by the addition of more broadly-ranging opposite-eye anticorrelations[17]. The monocularity and the growth rate of monocular patterns is enhanced at wavelengths equal to the peak of the fourier transform of the cortical interaction function. Introduction of anticorrelations within each eye can cause nonmonocular modes to grow fastest; but even in this case, the fastest-growing monocular modes and the most strongly monocular modes are found at the dominant wavelength of the cortical interaction function. Thus, the correlation function C^D provides the precondition for the ascendency of monocular cells. The cortical interaction function selects the wavelength of monocular cells that will grow the fastest, enhancing the growth rate and increasing the monocularity of those fastest-growing monocular patterns.

17. Opposite-eye anticorrelations also enhance the development of monocularity even if they do not extend more broadly than within-eye correlations. This is because their presence increases the rate of growth of S^D relative to the rate of growth of $S^S \equiv S^L + S^R$. This allows the development of ocular dominance segregation to proceed faster relative to the rate of topographic refinement of receptive fields and to the rate of approach of synapses to saturation.

Analysis of Limiting Cases These results can also be derived analytically through solutions of the equations in limiting cases. One simple limit is the case in which the correlation function C^D is constant over at least an arbor diameter plus the maximum distance x for which $I(x) \neq 0$. In this limit the influence between synapses depends only upon their eyes of origin and their cortical locations, and not upon their retinotopic locations. Then there can be no retinotopic refinement within each receptive field, since all synapses from a given eye onto a given cortical cell grow or decay identically. Hence, the only dynamical variable for each cortical cell is its ocular dominance.

The equation can be reduced in this limit to a simpler equation studied previously by Swindale (1980), by performing $\sum_\alpha$ on both sides of equation 5 to obtain

$$\frac{dD(x,t)}{dt} = \sum_y w(x-y)D(y,t) - \gamma D(x,t). \qquad (6)$$

$D(x,t) \equiv \sum_\alpha S^D(x,\alpha,t)$ is the ocular dominance of the cortical cell at x, $w(x-y) \equiv \lambda C^D NI(x-y)$ tells the influence between ocular dominance development at two different cortical locations, and $N \equiv \sum_\alpha A(\alpha)$ is the number of synapses in an arbor. Swindale called w(x–y) an "effective interaction", but its biological nature was not clear. In this limit, we may express his effective interaction in terms of correlations, arbors and intracortical interactions. Swindale's equation can be easily solved. It is a convolution. Hence, periodic modes of ocular dominance, $D_m(x) = e^{im \cdot x}$, grow with a rate ω_m determined by the fourier transform $\tilde{w}(m)$ of w(x), $\omega_m = \tilde{w}(m) - \gamma = \lambda CN\tilde{I}(m) - \gamma$. The full eigenfunctions of our original equation can also be found in this limit: for each m, there is one monocular mode, $S^D_m(x,\alpha) = e^{im \cdot x} A(x-\alpha)$, with growth rate ω_m as just given. The Swindale equation describes the growth of this mode. All other modes decay with growth rate $-\gamma$. Thus in this limit, the non-decaying eigenfunctions are completely monocular and the fastest growing mode is selected by the

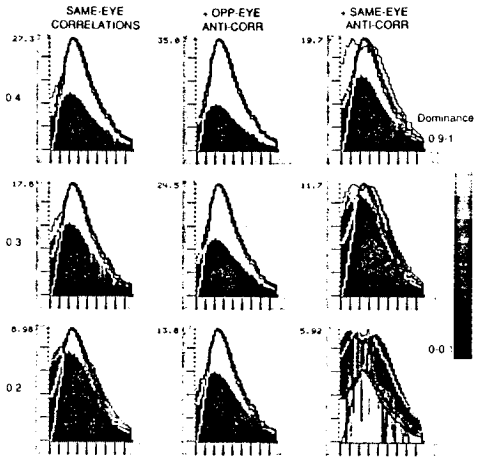

Figure 26: Computed growth rate (vertical axes) of characteristic patterns of ocular dominance, as a function of inverse wavelength of the pattern (horizontal axes). Results are presented for the nine correlation functions of figures 13 and 20, with Mexican hat cortical interaction function and flat arbor function as in those figures. Greyscale indicates the dominance of characteristic patterns: Dominance is a measure of the degree of monocularity of the pattern's characteristic receptive fields, on a scale from 0 for complete binocularity (black) to 1 for complete monocularity (light). Graphs for functions for which monocular patterns are the fastest growing (all but lower right) were constructed by painting lower dominance growthrates on top of higher dominance growthrates, so that the greyscale at any point reflects the lowest dominance patterns with wavelength corresponding to the point and growthrate at least as large as that corresponding to the point. For the case of "+ same-eye anticorrelations 0.2" (lower right), this scheme was reversed: Higher dominance growthrates were painted on top of lower dominance growthrates. Mixed black/white lines show the analytic predictions for growth rate as a function of inverse wavelength derived in limiting cases. Lower thin lines show the fourier transform of the cortical interaction function, which is the prediction in the limit of constant correlations; thick lines show the prediction of the broad correlations limit. These two predictions have been normalized to the maximum growth rate of patterns with dominance ≥0.5. The upper thin lines show the prediction of the limit of full connectivity, normalized to the maximum growth rate of any pattern. Number beside the vertical axis indicates the maximum growth rate of any pattern. The horizontal axis represents wave number; the wavelength in units of grid intervals is 25 divided by the wave number. The first bin on the horizontal axis represents wave numbers 0-0.23; subsequent bins represent increments of 0.4 in wave number, so that the second bin represents wave numbers 0.23 to 0.63, and so forth. From Miller, 1989c.

peak of $\tilde{I}(m)$. This limit is shown as the lower thin lines in figure 26. It accurately predicts the wavelength of the fastest growing monocular pattern, even far from the conditions in which the limit was derived.

In a limit of broad but not constant correlations, we approximate the correlation of one afferent with any afferent synapse onto a cortical cell, by the average correlation of that afferent with all afferent synapses onto that cortical cell. Thus, in equation 5, we set

$$C^D(\alpha-\beta)S^D(\beta,y) \approx \frac{\sum_\delta C^D(\alpha-\delta)A(\delta-y)}{\sum_\delta A(\delta-y)} S^D(\beta,y).$$

In this limit, the influence between synapses depends on the retinotopic location of the influenced synapse, but not of the influencing synapse. This limit also yields a Swindale equation after performing $\sum_\alpha$ on both sides, but now $w(x-y)=\lambda A*C*A(x-y)I(x-y)/N$. The '*' indicates convolution, $X*Y(z)=\sum_k X(z-k)Y(k)$, and $N=\sum_\alpha A(\alpha)$. The growth rates of cortical ocular dominance in this case are $\omega_m=(\lambda/N)\sum_k \tilde{I}(m-k)\tilde{A}^2(k)\tilde{C}(k)-\gamma$. Because C is assumed positive over a broad range, and because biologically A and C are likely to extend without oscillation over a much broader range than I, fourier transforms of A and C will be much narrower than that of I. This expression for ω_m then implies that the peak growth rate is found at or very near the m that maximizes $\tilde{I}(m)$, but the growth rates do not fall to zero as sharply as $\tilde{I}(m)$. This prediction is shown as the thick lines in figure 26. It accurately predicts the growth of monocular patterns of all wavelengths, even far from the limiting conditions in which it was derived.

A third relevant limit is the limit of complete geniculocortical connectivity, $A(x-\alpha)\equiv 1$, in which every geniculate cell is connected to every cortical cell. In this limit the eigenfunctions are $S^D_{k_x k_\alpha}(x,\alpha)=e^{ik_x x}e^{ik_\alpha \alpha}=e^{imx}e^{-ik_\alpha(x-\alpha)}$, with $m=k_x+k_\alpha$. The resulting growth rates are $\omega_{k_x k_\alpha}=\lambda\tilde{I}(k_x)\tilde{C}^D(k_\alpha)-\gamma$. The correlation function drives an oscillation across the receptive field with wavenumber k_α and growth rate proportional to $\tilde{C}^D(k_\alpha)$. For the fastest growing mode to be monocular, the peak of C^D must be at frequency 0. The cortical interaction function drives an oscillation across an arbor with wavenumber k_x and growth rate proportional to $\tilde{I}(k_x)$. The resulting

cortical oscillation wavenumber, m, is the sum of k_x and k_α. In the event of monocular modes, $k_\alpha = 0$, the arbor and cortical oscillations are identical. Therefore the peak of $\tilde{I}$ selects the fastest growing cortical wavelength of monocular modes. In general, the intuitive picture found in this limit, that correlations drive oscillations across a receptive field, intracortical interactions drive oscillations across an arbor, and the cortical oscillation is the sum of these two oscillations, is a useful one for understanding a wide variety of cases.

In this limit, the fastest growth rate for a pattern with a given wavenumber m is proportional to the maximum over all k_α of $\tilde{I}(m-k_\alpha)\tilde{C}^D(k_\alpha)$. The resulting predictions for fastest growth rate versus wavenumber m are shown as the upper thin lines in figure 26. When the peak of C^D is at frequency zero, this limit accurately predicts the growth rates of monocular patterns of each frequency. Otherwise, if the peak of C^D is at a wavelength less than about an arbor diameter, binocular patterns become dominant. Then this limit appears qualitatively to predict some aspects of the shape of the curve of fastest growth rates vs. wavelength for these binocular patterns.

We can summarize the results found by computation, and suggested by these limiting cases and other analytical methods, as follows. When same-eye correlations are locally greater than opposite-eye correlations, and not significantly less within an arbor radius, then C^D is locally positive, and nonnegative within an arbor radius. Under these conditions, monocular cells will tend to form. The width of dominance patches will then be determined by the dominant wavelength in the cortical interaction function, which is the peak of its fourier transform. A broader C^D leads to an increased dominance in growth rate of monocular over binocular patterns and thus an increase in the tendency to monocularity. Oscillations within C^D cause a tendency to oscillation of ocular dominance within individual receptive fields, and if present significantly within an arbor radius is inconsistent with monocular segregation.

The Role of Constraints There is one important addition to the above conclusions. For monocular patterns with wavelength longer than an arbor diameter to grow, entire arbors centered within ocular dominance patches must either grow or shrink. If this were the case, some regions of the visual field in each eye would come not to be represented at all in the cortex. Hence, one might expect that the

growth of such patterns is somehow prevented in biological systems. This could occur dynamically, if biological parameters select patterns with wavelengths shorter than an arbor diameter. Alternatively, these patterns might otherwise tend to grow, but be suppressed by additional limitations on development. For example, a presynaptic cell whose terminal arbor has a smaller total synaptic strength may compete more effectively for its remaining synapses, while one with more total synaptic strength may become less competitive or reach limits to its ability to support further synaptic strength. This would yield a constraint on the total synaptic strength supported by a presynaptic cell.

Such a constraint can be modelled by fixing the total synaptic strength over a presynaptic arbor. The effect, as suggested, is to prevent the growth of monocular patterns longer than an arbor

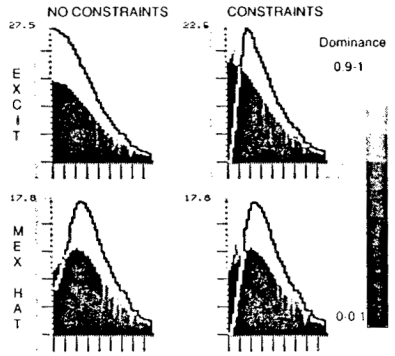

Figure 27: Computed growth rate (vertical axes) of characteristic patterns of ocular dominance, as a function of inverse wavelength of the pattern (horizontal axes), for the two cortical interactions and the two choices of constraints on afferent arbors of figure 21. Mixed black/white lines indicate predictions of the broad correlations limit, described in the text. Conventions otherwise as in figure 26. The constraints suppress the growth of monocular patterns with wavelength longer than an arbor diameter. This has a profound effect on the outcome when the excitatory cortical interaction function is used, selecting a wavelength of about an arbor diameter. There is little effect when the mixed excitatory/inhibitory interaction function is used, because that function normally selects a wavelength shorter than an arbor diameter. Maximum growth rates are at wavelengths of 7.3-8.3 grid intervals (excitatory function, with constraints) or 5.4-5.9 grid intervals (Mexican hat function). From Miller, 1989c.

diameter (figure 27). If the cortical interactions select a pattern with a wavelength shorter than an arbor diameter, the constraints have essentially no effect on the overall pattern that develops. However, if the cortical interactions select a pattern with longer wavelength, as in the case of purely excitatory cortical interactions, the effect is dramatic: the constraints force selection of a wavelength of about an arbor diameter. This was demonstrated in simulations in figure 21.

Mathematically, the constraint on presynaptic cells is modelled as follows. Write equation 5 as $\frac{dS^D(x,\alpha,t)}{dt} = LS^D(x,\alpha,t)$ as previously, and let $\gamma=0$. Now replace this equation with $\frac{dS^D(x,\alpha,t)}{dt} = LS^D(x,\alpha,t) - \kappa\frac{A(x-\alpha)}{N}\sum_y LS^D(y,\alpha,t)$ where $N \equiv \sum_x A(x-\alpha)$, with $0 \le \kappa \le 1$. Setting $\kappa=0$ gives the original equation. Setting $\kappa=1$ yields a fully constrained equation for which $\sum_x \frac{dS^D(x,\alpha,t)}{dt} = 0$, as would be the case if total synaptic strength over afferent arbors were fixed. In the constant correlations limit, the result of this extra term is to multiply the m-dependent part of the growth rate for monocular modes by $1-\kappa\frac{|\tilde{A}(m)|^2}{|\tilde{A}(0)|^2}$. This suppresses monocular modes whose oscillation frequency m contributes significantly to $\tilde{A}$, that is, modes whose wavelengths are longer than an arbor diameter. In the broad correlations limit, a similar result is obtained: the monocular growth rates become

$$\omega_m = (\lambda/N)\sum_k \tilde{I}(m-k)\,\tilde{A}^2(k)\tilde{C}(k)\left[1-\kappa\frac{\tilde{A}(m)}{\tilde{A}(0)}\frac{\tilde{A}(k-m)}{\tilde{A}(k)}\right] \qquad (7)$$

Similar results are obtained by modeling the constraint as subtraction of a term $-\kappa'\sum_x S^D(x,\alpha)$, or as combinations of the two terms. Other methods of analysis of these equations also support this conclusion: that constraints serve to suppress the growth of monocular modes whose wavelengths are longer than an arbor width, or more specifically, long enough to contribute significantly to $\tilde{A}$.

Constraints on the total synaptic strength supported by a postsynaptic cell may also play an important role. Biologically, one expects neither that all geniculate synapses onto a cortical cell will decay in strength, resulting in a loss of all visual input, nor that all geniculate synapses onto a cortical cell will grow in strength, leading to hyperresponsiveness and loss of selectivity. Rather, one expects that there will be a competition, by which some patterns of input grow in synaptic strength at the expense of other patterns. Such competition may occur dynamically, or it may be imposed through conditions that limit the total synaptic strength over a cortical cell. Such postsynaptic constraints can be imposed on the equation for the sum of the two eyes' synaptic strengths, $S^S \equiv S^L + S^R$, without effect upon the equation for S^D. Hence, such constraints can be imposed without effect on the development of ocular dominance periodicity.

In summary, given a correlation function that encourages monocularity, the width of a cycle of right-eye plus left-eye ocular dominance patches is determined by the dominant wavelength in the cortical interaction function, up to a limit set by the arbor width and by constraints on total afferent strength. If the cortical interaction function would drive a longer wavelength, constraints on presynaptic cells can select a wavelength set by the arbor diameter.

Comparison of Predictions to Simulated Results We can test the analytical understanding of the model by comparing the period of ocular dominance segregation that emerges in simulations with the predictions made by analysis. To measure the period in the simulated cortex, we examine the relative contributions of each wavelength to the cortical patterns of ocular dominance by measuring the power spectrum of these patterns[18]. Figure 28 shows the time development of the power (vertical axis) at each inverse wavelength (horizontal axis) in the development of a cortical pattern of ocular dominance from a random initial condition. These are the power spectra of the cortical patterns of ocular dominance shown in figure 14. The prediction of growth rate versus inverse wavelength in the broad correlations limit is presented as the grey background to each graph.

18. We compute the 2-dimensional fourier spectrum of the pattern of ocular dominance in the simulated cortex. We then determine the average power in small annuli in 2-D fourier space, representing small increments of wavelength.

Early in development, when the equations are linear, the fastest-growing wavelength is predicted perfectly by the broad correlations limit. The nonlinearities can result in small shifts in the final wavelength, in this case by allowing a fast-growing wavelength that dominated the random initial condition to remain dominant.

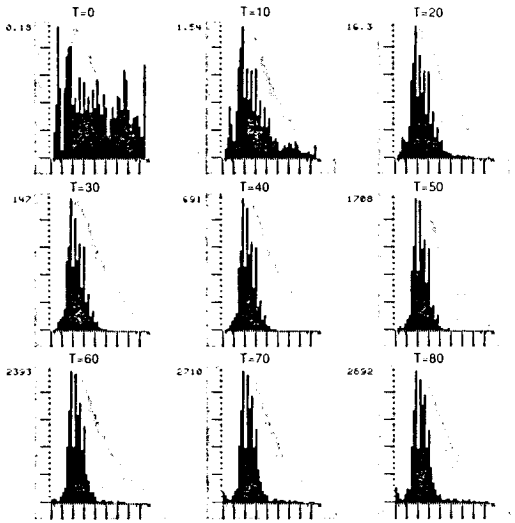

Figure 28: Development of the power (vertical axis) at each inverse wavelength (horizontal axis) in the cortical patterns of ocular dominance that develop in simulations. Power is black, compared to the analytical prediction of the limit of broad correlations, grey. These are the spectra of the cortices shown in figure 14. The number along the vertical axis shows the maximum power present in any wavelength bin at the given time, on a scale which is arbitrary but consistent across the various spectra presented. The binning of the horizontal axis is as described in figure 26. Note that each bin has a width of 0.4 grid intervals in Fourier space, so a difference of two bins represents a difference of less than one Fourier grid interval. From Miller, 1989c.

The power spectra of the final cortices that result from varying the correlation, cortical interaction, and arbor functions yield similar results (Miller, 1989c). The dominant wavelength in each final cortex is well predicted by the analysis, except when anticorrelations within each eye disrupt the overall monocularity.

Though the power spectra resulting from simulations are like those predicted, the precision is not sufficient to closely predict a wavelength. The wavelengths representing peak power are generally found within ±1 grid interval in Fourier space of the predicted peak, while almost all of the power in the final pattern is found within ±1.8 grid intervals in Fourier space of the predicted peak[19]. Using the Mexican hat cortical interaction function and the flat arbor function, these spans of inverse wavelength in Fourier space correspond in real space to wavelengths of 5.4±1.1 grid intervals and 6.05±2.25 grid intervals, respectively. This lack of precision may be related to the coarseness of the grid: wavelengths represent only a small number of grid intervals, so that uncertainty of only a few grid intervals corresponds to a significant variation of wavelength. One can guess that the precision of prediction may be greater when there are many grid intervals to a wavelength. Assuming a horizontal spacing of roughly 20 μm between cortical cells in layer 4, there are perhaps 30-40 cortical cells across one wavelength of right-eye plus left-eye patches in the cat or monkey visual cortex.

On What Do the Model Results Depend? Development of a periodic pattern of ocular dominance is an extremely robust phenomena, dependent only upon the three basic functions of the model, and perhaps on constraints on afferent arbors. However, the full expression of these tendencies depends upon the implementation of the model: on the limits on synaptic strengths, both of individual synapses and of total strengths over an afferent or over a cortical cell; and also on additional nonlinearities.

The analysis of periodicity examined only the development of the *difference* between the two eyes' synaptic strengths. However, the details of receptive field and afferent arbor structure depend also upon the development of the *sum* of the two eyes' synaptic strengths. For example, if the sum is growing everywhere, so that each eye's strength

19. The histograms showing power versus inverse wavelength are binned so that ±2 bins about the peak bin corresponds to a span of ±1 grid intervals in wavenumber, while ±4 bins about the peak bin corresponds to a span of of ±1.8 grid intervals in wavenumber. Details of the binning are found in the legend to figure 26.

is growing everywhere, then although a periodic difference in the strength of the two eyes may develop, this periodic pattern does not result in segregation. If this occured, individual receptive fields could show dominance, but they would not be monocular; similarly, individual afferent arbors could show periodicity, but they would not be confined to periodic patches. It is possible that there would be no final periodicity at all. For example, if all synapses tended to grow, and there were no constraints limiting total synaptic strength either over afferents or cortical cells, all synapses from both eyes would grow to saturation. Then periodicity would be manifest only during development, in the differing rates of reaching saturation. By using constraints that conserve total synaptic strength over each cortical cell, we avoid such problems without affecting the development of a periodic pattern in ocular dominance.

Similarly, receptive fields tend to focus their strength centrally in the model, provided that correlations are positive within each eye and diminish over less than an arbor width. The reason is that central synapses in the receptive field then have a larger number of correlated neighbors than do peripheral synapses, and hence tend to grow more quickly. Without a constraint on the total synaptic strength over a cortical cell, however, this refinement might in the end disappear as the fastest-growing synapses saturate and the slower-growing, more peripheral synapses catch up.

Biologically, there must be some limits on synaptic strengths, but very little is known about what they are or how they are implemented. Many means of achieving such limits have been used in previous models. Two broad classes can be distinguished (Miller, in preparation): multiplicative (von der Malsburg, 1973; Oja, 1982), and subtractive (Bienenstock, Cooper, and Munro, 1982; Linsker, 1986a-c; Miller, Keller, and Stryker, 1989; Sejnowski, 1977). In multiplicative methods, total synaptic strength over a cell is limited or conserved by multiplying each synapse on the cell by a constant determined after each iteration. In subtractive methods, each synapse on the cell has a constant subtracted from it, the constant determined after each iteration. There are important differences between these two methods. In multiplicative methods, ocular dominance segregation cannot occur in the absence of anticorrelations between the eyes[20]. This seems overly restrictive for study of the ocular

dominance system. With subtractive methods, such as the one we use, there is no such requirement. With multiplicative methods, final synaptic strengths tend to be proportional to a synapse's average activity when the cortical cell is active, so that for example topographic refinement will manifest in a gradual decrease in synaptic strengths from the center to the periphery of a receptive field. With subtractive methods, final synaptic strengths tend to all be saturated at the maximum or minimum allowed values. In this respect, multiplicative methods might make easier the modeling of systems such as the somatosensory cortex which remain subject to activity-dependent plasticity throughout adulthood.

The robust features of the model are those involving relative rates of growth: the tendency of one eye's synapses to grow faster than another's on a cell, or of central synapses on a cell to grow faster than peripheral ones. These robust features result from interactions among synapses, and the correlations between them. The less robust features of the model involve absolute rates of growth. These are determined by the constraints, and do not depend on specific interactions between synapses. Biologically, robust tendencies to the development of monocularity, the organization of a periodic pattern of ocular dominance, and the refinement of receptive fields do exist, and it appears that sufficient constraints exist to ensure that these tendencies are fully expressed. Except for the differences outlined between subtractive and multiplicative methods, the results of development do not appear to depend greatly upon the method of limiting synaptic strengths. Hence, in the absence of experimental knowledge, we prefer to use the simplest possible model of constraints.

---

20. Multiplicative conservation of the sum of synaptic strengths over a cortical cell reduces that sum at each iteration by an amount proportional to its growth rate. Hence, if the growth rate of the difference of synaptic strengths between the two eyes is smaller than the growth rate of the sum of synaptic strengths in the absence of constraints, the difference of synaptic strengths between the two eyes will end up shrinking after application of multiplicative constraints. The growth of the difference is driven by the correlation function $C^D = C^{SameEye} - C^{OppEye}$, while the growth of the sum is driven by $C^S = C^{SameEye} + C^{OppEye}$. Therefore, in order for the difference to grow faster than the sum, there must be opposite-eye anticorrelations.

Discussion

Biological Implications of the Model Results We have shown that many phenomena associated with ocular dominance segregation are implicit in a Hebbian synapse mechanism and in other mechanisms involving synaptic reward via correlated activity. These phenomena emerge provided that afferents from a single eye are locally correlated in their activities, and that there are interactions across cortex by which synapses may influence one another's growth. This simple framework can account for the development of monocular cells and their organization into periodic patches or columns, the topographic refinement of receptive fields, and the confinement of afferent arbors to patches. Correlations of inputs over about ½ of an afferent arbor radius, as may be the case for X-cells in the cat (based upon measurements in adult cat: Humphrey et al., 1985a,b; Mastronarde, 1983a,b; Tusa, Palmer, and Rosenquist, 1978), can lead to a layer 4 with many binocular cells at the borders between patches, as observed in the cat (LeVay, Stryker, and Shatz, 1978). Broader correlations can lead to a virtually completely monocular layer 4, as is seen in the monkey (Hubel, Wiesel, and LeVay, 1977). The effects of experimental manipulations of activity, including monocular deprivation (Hubel and Wiesel, 1970; Wiesel and Hubel, 1965), strabismus or alternating monocular deprivation (Hubel and Wiesel, 1965), and cortical infusion of muscimol (Reiter and Stryker, 1988), all follow naturally from the model, and a critical period for these effects emerges.

The model can also account quantitatively for the width of the ocular dominance organization that develops. The observed period of this organization (width of right-eye plus left-eye patch) in the cat is 850 μm (Anderson, Olavarria, and Van Sluyters, 1988; LeVay, Stryker, and Shatz, 1978; Shatz, Lindstrom, and Wiesel, 1977; Swindale, 1988). To understand how a simple intracortical interaction might yield this wavelength as the peak of its fourier transform, it is helpful to keep two thoughts in mind. First, if a function is excitatory over a radius of about 200 μm, and strongly inhibitory more distantly, it can have this desired 850 μm peak. For example, a cosine wave with wavelength 850 μm is positive for ±212 μm from 0, then equally inhibitory over the same distance more peripherally. Second, a function can be excitatory over a much smaller region, and retain the same fourier peak, if the inhibition is made correspondingly weaker. For example, if there is no inhibition at all, the peak wavelength of an excitatory region of any size is at an infinitely long wavelength. Hence, functions excitatory over radii of 50 or 100 μm, with weak inhibition more peripherally, can also yield the desired wavelength.

As previously observed, we do not know enough about the nature of the intracortical interaction in general, and in particular at the time of ocular dominance segregation, to compare it to the 850 μm period in a precise way. We can only say that the distances over which excitation and inhibition are seen in the adult seem consistent with this period (Hata, et al., 1988; Hess, Negishi and Creutzfeldt, 1975; Toyama, Kimura, and Tanaka, 1981a,b; Worgotter and Eysel, 1989). If in addition there are longer-range interactions with a preexisting period on the order of 850 μm (Gilbert and Wiesel, 1983; Luhmann, Martinez Millan and Singer, 1986; Tso, Gilbert, and Wiesel, 1986; Worgotter and Eysel, 1989), this could create, or add to, a peak in the fourier transform at this wavelength.

If the intracortical interaction is purely excitatory, or otherwise selects a wavelength longer than an initial afferent arbor diameter, constraints can lead to wavelength selection by the arbor function. An 850 μm period can be selected by an arbor function that either is uniform over a diameter of 850 μm, or tapers over a somewhat larger diameter. Hence, it seems possible that X-cell afferent arbors could by this limiting mechanism be responsible for the wavelength of ocular dominance (based on maximum extent of patchy adult arbors: Humphreys et al., 1985a,b). However, Y-cell afferent arbors are likely to be be too large to play such a role (Humphreys et al., 1985a,b; LeVay and Stryker, 1979). It is interesting in this context that several experiments suggest that the X-cell projection develops earlier than that of the Y-cells (Sherman and Spear, 1982), and so might play a dominant role at the time of ocular dominance segregation.

The most obvious experiment suggested by the model is to better characterize the nature of the three functions at the onset of ocular dominance segregation. Measurement of initial correlation, cortical interaction, and arbor functions in various brain regions or species can test whether a proposed developmental mechanism is consistent with the periodicity that emerges in each case. Comparisons across such regions or species can enhance insight. For example, ocular

dominance patches in area 18 of the cat are more than 1.5 times wider than those in area 17; arbors, and perhaps correlations, are also more widespread (Anderson, Olavarria, and Van Sluyters, 1988; Humphrey et al., 1985a,b; Lowel and Singer, 1987; Shatz, Lindstrom, and Wiesel, 1977; Swindale, 1988). If a Hebb mechanism is responsible for ocular dominance segregation in these two areas, two possibilities arise. First, intracortical connectivities in kittens may be sufficiently different between the two regions to account for the difference in patch width. Alternatively, both regions in kittens might have predominantly excitatory intracortical connections, resulting in arbor-limited patch widths. If measurement were to establish that neither of these possibilities is the case, one would conclude that the patch width is not likely to be determined by a Hebbian mechanism.

Sustained perturbation of the three functions in an experimental preparation beginning before the normal onset of segregation, and comparison of the resulting periodicity to the unperturbed case, can also test mechanisms. Under the hypothesis that a Hebb mechanism underlies ocular dominance development, periodic segregation is driven by intracortical synaptic connections. Local infusion of muscimol, an agonist of $GABA_A$ receptors which inhibits postsynaptic cells, will eliminate activation of such connections. We therefore would predict that no pattern of ocular dominance organization would be seen in a cortical regions into which muscimol was infused, although individual cells might become monocular. Alternatively, intracortical inhibitory connections may be blocked by local infusion of bicuculline, an antagonist of GABA receptors. A resulting increase in patch period would be consistent with the hypothesis that the underlying mechanism is Hebbian and that the patch width is determined by the intracortical interactions. If patch period were unchanged by bicuculline, one would conclude either that the period was normally arbor-limited (which could be tested by measuring whether intracortical interactions were predominantly excitatory during initial column development) or that a non-Hebbian mechanism was involved.

The model predicts that broader correlations within each eye would increase monocularity of layer 4 for mechanisms of the type we study. This could be tested by inducing broader correlations through pharmacological interventions in the retinas. One could also measure whether retinal correlations are broadened in animals deprived of pattern vision. Such animals have increased numbers of monocular cortical neurons (Sherman and Spear, 1982). Finally, one could measure whether geniculate correlations are broader, relative to a geniculocortical arbor radius, in developing monkeys than in kittens, since layer 4 is fully monocular in adult monkeys (Hubel, Wiesel, and LeVay, 1977) but not in cats (LeVay, Stryker, and Shatz, 1978).

In sum, the model suggests that much of the known phenomena of ocular dominance segregation follow from simple dynamics common to a number of proposed mechanims. It does not allow us to specifically distinguish one mechanism from another on the basis of existing experiments. It does, however, provide a framework for experiments capable of making such distinctions. In particular, it seems feasible to distinguish between mechanisms that would determine the period of segregation on the basis of intracortical synaptic connectivity, and mechanisms that determine a period on the basis of either afferent arbor diameter or intracortical interactions that involve diffusion rather than synaptic connections.

Implications for Other Models of Cortical Development and Plasticity

The present work extends previous theoretical studies of ocular dominance column development. Von der Malsburg and Willshaw, in a series of papers in the 1970's, demonstrated through computer simulation that mechanisms like those discussed here were sufficient to yield stripes as well as topographic maps (von der Malsburg, 1979; von der Malsburg and Willshaw, 1976, 1977; Willshaw and von der Malsburg, 1976, 1979). Bienenstock, Cooper and Munro (1982) focused on the development of monocularity in isolated cortical cells, as well as on dynamical means of limiting synaptic strengths, but did not study cortical organization.[21] Legendy (1978) studied a Hebb-like model, and concluded that intracortical synaptic interactions will determine the distances over which cortical cells are similar in their response properties. Swindale (1980) formulated a model in terms of an effective interaction between right-eye and left-eye synapses,

21. The relationship of the present model to the model of Bienenstock, Cooper, and Munro is discussed in detail in Miller, 1989a,c.

which produced stripes like those obtained here. This interaction was not related to measurable biological quantities. In the limit in which correlations among afferents vary slowly over an arbor radius, our model can be reduced to his, allowing us to express his effective interaction in terms of arbors, cortical interactions and afferent correlations.

Two models of cortical development discussed elsewhere in this volume may be compared to the model presented here. These are the models of Linsker (1986a-c, and Chapter 10)[22] and of Pearson, Finkel, and Edelman (1987, and Chapter 7). We will discuss these models in some depth, with the intents both of clarifying the similarities and differences between the models, and of illustrating how our methods can yield insight into the behavior and meaning of these models.

Linsker's Model of Development of Orientation Selectivity

Linsker (1986a-c, and Chapter 10) developed a model of plasticity very much like ours. He used it to study the development of orientation selectivity in visual cortex. He initially studied the development of a single, isolated postsynaptic cell, and considered inputs from only a single eye. He assumed a gaussian arbor function, but one can formulate his model in terms of a general arbor function. Let α represent the location of the presynaptic cell, relative to a postsynaptic cell at x=0. Then Linsker's equation, after explicit inclusion of the arbor function, can be written

$$\frac{dS(\alpha,t)}{dt} = A(\alpha)\left\{\sum_\beta \frac{C(\alpha-\beta)}{N} S(\beta,t) - k_2[\bar{S}(t) - S_{TARGET}]\right\}$$

where $N=\sum_\alpha A(\alpha)$, $\bar{S}(t)=\frac{\sum_\alpha S(\alpha,t)}{N}$, $S_{TARGET}=k_1/k_2$ in Linsker's notation, and k_1 and k_2 are constants that Linsker defines[23]. $S(\alpha,t)$ is

22. We will be concerned here only with Linsker's work on the development of orientation selectivity in visual cortex (Linsker, 1986a-c), and not with the later work on information theory, which comprises much of his chapter in this volume.

23. We have changed the sign of k_2 compared to Linsker's equation so that the negative sign in front of k_2 can be seen explicitly. Linsker uses a positive sign, but a k_2 that is negative.

allowed to range between $-0.5A(\alpha)$ and $0.5A(\alpha)$.

Linsker's model differs from ours in several important respects. First, in his model modifiable synapses S may have either positive or negative strength, whereas we require input synapses to have positive strengths. Note that in our model, the variable S^D, the ocular dominance or difference between the two eye's strength, may become either positive or negative. Hence, we can mathematically use our analysis of S^D to understand Linsker's S.

Linsker offers two possible interpretations of the positive and negative synapses. In one interpretation, each individual synapse may become positive or negative. In contrast, biological synapses are either exclusively excitatory or exclusively inhibitory. In the alternative interpretation, there are equal numbers of excitatory and inhibitory synapses, with identical spatial distributions and connectivities, and with indistinguishable statistics of activation so that an excitatory input is equally correlated to either an excitatory or an inhibitory input at a fixed distance. Furthermore the excitatory and inhibitory populations obey mirror-image plasticity rules, so that excitatory synapses are strengthened by correlation between postsynaptic and presynaptic activity and weakened by anticorrelation, while negative synapses are equally weakened (made less negative) by correlation and strengthened by anticorrelation. These conditions together mean that the "excitatory" and "inhibitory" populations are just positive and negative halves of a single statistical population. The geniculocortical projection is exclusively excitatory, so this second interpretation is also ruled out for that projection. The projection in monkeys from the unoriented cells of layer 4C to the oriented cells of the upper cortical layers includes both excitatory and inhibitory inputs, but it is likely that the two populations are distinct in crucial ways. For example, inhibitory cells are often interneurons which, when active, inhibit nearby excitatory cells, so that the inhibitory and excitatory populations would be expected to have statistically distinct firing patterns. Similarly, while there is extensive evidence that excitatory synapses can be modified in a Hebbian manner (Nicoll, Kauer, and Malenka, 1988), current evidence suggests that there may be little modification of inhibitory synapses under the same stimulus paradigms (Abraham, Gustafsson, and Wigstrom, 1987; Griffith, Brown and Johnston, 1986).

We have offered a third alternative intepretation of the negative

synapses (Miller, 1989b). ON- and OFF-cells are known, in adults, to be anticorrelated with one another over distances similar to those over which each individual cell type is correlated (Mastronarde, 1983a,b). Consider populations of ON-center and OFF-center cells making strictly positive synapses onto cortex and having identical spatial distributions (which is at least approximately biologically correct). Suppose they are exactly anticorrelated with one another, so that $C^{ON:ON}(\alpha)=C^{OFF:OFF}(\alpha)=-C^{OFF:ON}(\alpha)$. Then the mathematics of Linsker's model of an "excitatory" and "inhibitory" population is identical to the mathematics of these ON- and OFF-cells, except for the important distinction that different constraints are needed[24]. One can relax the requirement of anticorrelations being exactly equal and opposite to the correlations without substantially altering the results.

Second, Linsker's model differs from ours in using constraints that ultimately fix both the summed excitatory and the summed inhibitory input to a cortical cell. In our model, the summed excitatory input is fixed, and the inhibitory input is fixed at zero. However S^D, the variable in our model that can be either positive or negative and hence is mathematically analagous to Linsker's, is unconstrained in its total onto a cortical cell; instead we consider the effect of constraints on the total that comes from each geniculate location. Linsker's constraints emerge as follows: the effect of the second term in $\frac{dS}{dt}$, for sufficiently large k_2, is to constrain S so that $\bar{S}(t)\approx S_{TARGET}$. If one begins in a condition in which the constraint is not satisfied, and if k_2 is sufficiently large (as Linsker's k_2 is), the second term in $\frac{dS}{dt}$ dominates the term involving correlations. Then

24. See description of Linsker's constraints in next paragraph in text. ON- and OFF-center geniculate cells appear to be entirely identical histologically, and are distinguished only by their inputs and their patterns of neural activity. Therefore, the postsynaptic cell could not separately limit the synaptic strength of each type of input. Thus, it is not appropriate to fix the total ON-synaptic strength and the total OFF-synaptic strength onto each cortical cell, which would be equivalent to Linsker's constraints. If one assumes that each geniculate afferent maintains a fixed amount of synaptic strength, one would then constrain the total ON-synaptic strength and the total OFF-synaptic strength coming from each geniculate location. This is the type of constraint we used for S^D.

either all synapses increase in strength, or all synapses decrease in strength, until the constraint is satisfied. Furthermore Linsker shows that development will continue on a single cell until all, or all but one, synapses are at their maximum or minimum allowed value, $\pm 0.5A(\alpha)$. Hence in the final state $\sum_\alpha |S(\alpha)| \approx 0.5N$, while $\sum_\alpha S(\alpha) \approx NS_{TARGET}$. From this, one can conclude that in the final state $\sum_{\alpha:S\,excitatory} S(\alpha) \approx \frac{N}{2}(0.5+S_{TARGET})$, $\sum_{\alpha:S\,inhibitory} S(\alpha) \approx -\frac{N}{2}(0.5-S_{TARGET})$. Linsker's model thus separately fixes the final total excitatory and total inhibitory synaptic strengths.

Our eigenfunction analysis of S^D can provide insight into his results. Linsker starts with a layer of cells whose activities are uncorrelated. He sets $S_{TARGET} > 0.5$, which causes each synapse to grow independently until it reaches its maximum positive strength. The resulting postsynaptic cell is thus an "all-excitatory" cell. In a layer of such cells whose inputs have overlapping gaussian arbors, neighboring cells will receive common excitatory inputs and thus be correlated in their activity. The degree of correlation between two cells will be proportional to the degree of overlap of their inputs and, hence, will decrease with the distance between the two cells in a gaussian manner. Next, a layer of such cells sends inputs to a subsequent layer, and S_{TARGET} is set somewhat less than 0.5 so that a significant number of synapses are forced to become negative. In this case, "center-surround" cells develop. This can be understood simply from the fact that the fastest-growing eigenfunctions for S^D, for a gaussian correlation function (i.e., "same-eye correlations"), have receptive fields that concentrate their strength centrally. When combined with constraints that, for example, force 35 percent of final synaptic strength to be negative ($S_{TARGET}=0.15$), this can lead to a center of positive synapses with a surround of negative synapses[25]. Hence, formation of these "center-surround" cells depends critically on the negative synapses and the constraints. The robust feature is that central synapses grow faster than peripheral ones.

25. A thorough analysis of this process will be found in D.J.M. MacKay and K.D. Miller, in preparation.

A layer of such center-surround cells, if all cells have identical phase (positive centers, negative surrounds), has a "Mexican hat" correlation function: nearby cells have correlated patterns of activity, while more distantly spaced cells in the layer are anticorrelated with one another. Nearby cells are correlated because they receive common excitatory inputs. More distantly spaced cells have overlap between one's excitatory center and the other's inhibitory surround, and thus anticorrelated firing. The development of anticorrelations in the afferent correlation function thus depends upon the development of "center-surround" cells, which in turn depends upon both the negative synapses and the constraints.

Linsker uses repeated layers with similar values of S_{TARGET} to obtain repeated layers of cells that are "center-surround" in terms of the previous layers, and that have identical phase. This strengthens the anticorrelations between more distant cells in each subsequent layer, and introduces further oscillations in sign of the correlation function with increasing distance between cells. Retinal ganglion cells and cells in the LGN and, in monkeys, layer 4C of cortex have center-surround receptive fields in terms of the visual field. However, Linsker's mechanism for strengthening of anticorrelations requires that geniculate cells have center-surround receptive fields in terms of retinal ganglion cells, so that the center responses of geniculate cells originate from the center responses of one set of retinal ganglion cells, and the surround responses of geniculate cells originate from the center responses of surrounding retinal ganglion cells; or similarly, that monkey 4C cells have center-surround receptive fields in terms of geniculate cells. There is as yet little evidence on whether either of these is the case.

Given an afferent correlation function with strong anticorrelations, and a sufficiently broad arbor function so that inputs in the center of the receptive field "see" a substantial number of anticorrelated inputs, oriented cells develop. Linsker found that multibanded oriented cells will develop, that is cells with a central band of synapses flanked by one or more side bands of alternating sign. Development of such multilobed structures appears to depend upon both multiple oscillations of sign in the correlation function, and on very fine tuning of the constraints (unpublished observations). However, we have seen that if a Mexican hat correlation function is sufficiently narrow with respect to the arbor function, the fastest-growing receptive field pattern has a positive stripe adjacent to a negative stripe. Hence, development of an oriented cell consisting of two bands, one excitatory and one inhibitory, can occur simply with anticorrelations and in the absence of constraints. When multiple cells are connected into a cortical layer, an alternation of two-banded and three-banded structures can result, due to the oscillation in phase across cortex of the eigenfunctions of S^D (Miller, 1989b).

There are again several difficulties with interpreting these results biologically. First, it is not clear that orientated cells can be achieved either without negative synapses or without unrealistic assumptions about the statistics of activity of the positive and negative synapses[26]. If synapses are solely positive and the arbor function does not decrease with distance sufficiently quickly, central synapses grow more *slowly* than peripheral synapses in the presence of a Mexican hat correlation function, leading to bizarre receptive fields with synaptic strength confined to peripheral clumps. This occurs because central synapses then have more anticorrelated neighbors than peripheral ones. If the arbor function tapers with distance sufficiently quickly, central synapses will grow more quickly than peripheral ones, but the synapses tend to remain confined within the correlated central region in a circularly symmetric manner (Miller, 1989a,c). However, in some conditions it appears possible to obtain oriented cells by this mechanism with strictly positive synapses (Linsker, personal communication; Miller, 1989a,c)[27]. Second, when two eyes are present, anticorrelations among afferents within each eye will destroy monocularity (figure 26). A combination of same-eye and opposite-eye anticorrelations can eliminate anticorrelations from C^D, while

26. If our interpretation in terms of ON- and OFF-cells is utilized, this problem is avoided. However, it is replaced by another problem. Linsker's result requires ON-ON and OFF-OFF correlations to be positive among near neighbors and negative among more distant neighbors, while OFF-ON correlations are negative among near neighbors and positive among more distant neighbors. The changes of sign with distance have thus far not been observed.

27. If total synaptic strength is conserved by multiplication of each synapse by a constant, rather than subtraction from each synapse of a constant, after each iteration, at least weakly orientated cells can emerge (Miller, 1989a,c).

causing deep anticorrelations in the correlation function that drives development of the sum of the synaptic strengths of the two eyes, $C^S \equiv C^{LL} + C^{LR}$. Again, at least under special circumstances this can yield cells that are monocular and at least weakly oriented (Miller, 1989a,c).

Finally, returning to synapses that can be either negative or positive, suppose that a layer of such oriented cells develops in the presence of weak but long-distance excitatory connections between cells within the layer. Then Linsker has proposed an analysis showing that oriented cells will organize into a global arrangement of orientations that in certain respects closely resembles biological results found subsequently (Blasdel and Salama, 1986)[28]. He assumes that the excitatory connections are weak enough not to disturb the receptive field structure that develops in isolated cells, but strong enough to nonetheless organize these cells with respect to one another during development. The eigenfunction analysis presented here for S^D shows that, in the absence of constraints, even weak cortical interactions cause patterns to develop that oscillate in phase across cortex. That is, if one part of cortex has oriented receptive fields with an excitatory central band and inhibitory side bands, nearby parts of cortex would have receptive fields with an inhibitory central band and excitatory side bands. For this reason, Linsker's assumption that receptive field structure is not disturbed is not valid in the absence of his constraints. His constraints cause this oscillation to be suppressed by causing a pattern with infinite wavelength – no oscillation – to grow faster than other patterns. Hence, the cortical organization he finds also depends critically on his constraints (to be discussed in Miller and MacKay, in preparation). Such constraints are not present when the model is interpreted in terms of ON and OFF cells, so such an interpretation leads to different cortical organization of orientation than that proposed by Linsker (Miller, 1989b).

28. One point of discrepency is that Linsker's mechanisms leads groups of vertically oriented cells to be extended across cortex in the retinotopically vertical direction, and similarly for all other orientations. No such arrangement has been seen in several studies (Blasdel and Salama, 1986; Swindale, Matsubara, and Cynader, 1987).

In sum, Linsker's work has been of great importance in pointing out in general how significant organization of individual receptive fields, as well as of cortex as a whole, can arise from simple Hebbian mechanisms. In particular, Linsker pointed out that symmetry-breaking could occur, so that oriented receptive fields could arise from circularly symmetric arbors and correlations. It is important to understand the elements of the model that are responsible for each element of the results. This allows one to understand the specific results that might be biologically realistic. The development of center-surround organization and of anticorrelations in Linsker's model seems nonbiological, because of their dependence upon the negative synapses and the constraints. However, anticorrelations may arise by other means, and in particular, an interpretation in terms of ON and OFF-cells may provide a biological interpretation for some of the results on the development of oriented cells.

Pearson, Finkel, and Edelman's Model of Somatosensory Development Pearson, Finkel, and Edelman (1987; Chapter 7) developed a similar, but more complex, model to study somatosensory development and plasticity. We will discuss the model as presented in the 1987 paper. It is a "real-time" model, in that postsynaptic voltages develop and decay over time. Thus individual synaptic changes are followed, whereas our model only follows synaptic changes averaged over the ensemble of input patterns. The plasticity rule used by Pearson and colleages assumes that synapses are modifiable only during postsynaptic depolarization. Modifiable synapses tend to be converted from a weak to a strong form if sufficient "modifying substance," released by presynaptic activity, has accumulated; otherwise, they tend to be converted from the strong form to the weak form. Thus, synaptic plasticity occurs only with sufficient postsynaptic depolarization, and the sign of plasticity is then determined by the amount of presynaptic activity. The essence of the plasticity model can thus be expressed

$$\frac{dS(x,\alpha,t)}{dt} \propto f_1[POST(x)]f_2[PRE(\alpha)]$$

where POST is postsynaptic depolarization, PRE is presynaptic activity (both may have to be integrated over some relevant time), f_1 is

a function that is zero at or below resting potential and becomes positive with depolarization, and f_2 is a function that is negative for low presynaptic activities and positive for large presynaptic activities. In this form, it is easy to see that the model of plasticity is a particular form of a Hebbian rule. The most significant variation in this version is that the function of postsynaptic activity can never be negative. Such a variation was proposed by Stent (1973) but would seem to be contradicted in visual cortex by experiments that infuse muscimol to hyperpolarize postsynaptic cells, leading to an ocular dominance shift in favor of the *less* active eye (Reiter and Stryker, 1988), as was discussed previously.

The model has nearly 30 parameters, complicating analysis and rendering difficult the determination of the parameter regimes of which simulation results are representative. By considering the averaged changes to be expected in terms of the effective arbor function, correlation function and cortical interaction function, the present analysis can shed light on their results. The arbor functions used are identical: input cells connect to a 7×7 square arbor of excitatory cortical cells, with uniform connectivity within the arbor. The model of Pearson and colleagues uses two identical input grids, one representing glabrous and one representing dorsal input. These can equally be considered "right eye" and "left eye". The inputs are activated with 3×3 square stimuli, from which the average correlation in input can be easily calculated: within glabrous or dorsal, it is a function that is strictly positive and is nonzero over a square of ±2 gridpoints; between glabrous and dorsal, it is zero[29].

29. Glabrous and dorsal grids are actually connected on one side, so along this border there is some glabrous/dorsal correlation. Otherwise, with the sequential presentation of stimuli used in the model, the description given here of the correlation function is only strictly true in the limit of a large number of cells. Let correlations be defined as

$$C(\alpha,\beta)=\frac{1}{\#\text{stimuli}}\sum_{\text{stimuli}}[a(\alpha)-\bar{a}][a(\beta)-\bar{a}]=\frac{\sum_{\text{stimuli}}[a(\alpha)a(\beta)]}{\#\text{stimuli}}-\bar{a}\,\bar{a}$$

where $a(\alpha)$ is the activity of the input from α, and $\bar{a}$ is the mean activity (averaged over all stimuli) of each input. Let $a(\alpha)$ be 1 for stimuli in which the input at α is stimulated and zero otherwise. If two cells are simultaneously activated by stimuli centered at n cells, and individually activated by stimuli centered at 9 cells, out of N total cells stimulated, then this expression is $C(\alpha,\beta)=n/N-(9/N)^2$. When the number of cells N is large compared to 9, so that each cell's mean activity 9/N approaches zero, the description given in the text becomes accurate; since there were 1024 input cells, this is a very good approximation. The description of the correlation function in the text would also be true if stimuli were presented in parallel, with random times of activation at each site based on the mean activity of each.

In the model of Pearson and colleagues, significant synaptic changes occur over times short compared to the times in which all input patterns are activated. That is, a stimulus consisted of a prolonged set of activations (3 cycles of 6 steps on, 4 steps off) of a single 3-grid by 3-grid square. In one "pass" over the hand, a complete set of non-overlapping squares was sequentially given one such stimulus each. There were 4 passes. The 3×3 stimulus squares overlapped one another between passes, but not within passes. The result is that a local pattern could be formed during the prolonged stimulation of a single square, and during a pass in which only nonoverlapping squares are stimulated, rather than through an average over all stimuli. Because the size of such a local pattern is determined by the number of cortical cells activated by stimulation of a square, and this in turn should be determined by the intracortical interactions with the stimuli used, we have ignored this fact in our discussion.

The cortical interaction function must be estimated more roughly as there are many parameters underlying it[30]. Cortical cells are either excitatory (e) or inhibitory (i) cells. There are two excitatory and one inhibitory cortical cells at each point in the cortical grid. Input cells contact only e cells, and only the responses of e cells are studied. There are assumed to be e→e, i→e, and e→i intracortical connections. The e→e connections are themselves assumed to be modifiable by the same plasticity rule as the input synapses. Connectivity is established in terms of "square rings" of grid points around each point. At distances of 0–1 square rings, intracortical connections are strongly excitatory (that is, e→e connections are strongly dominant over [e→i→e] connections); at a distance of 2 square rings, connections are more weakly excitatory; and at greater distances (3 to 6 square rings), connections are exclusively inhibitory and extremely strong.

30. i cells are set to have much lower and much sharper thresholds then e cells. i cells produce shunting inhibition, so that a sufficient level of i-cell activation onto a cortical cell will prevent it from firing. e→e synapses are made 4.5 times more effective than e→i synapses or input synapses, and there are twice as many e cells as i cells.

The correlation function is essentially a "same-eye correlation" function nonzero over slightly less than an arbor radius. Therefore, one expects a largely or fully "monocular" cortex. That is, most cells should be largely or exclusively driven by either glabrous or dorsal inputs. This is found: 94 percent of nonboundary cells in the simulation presented are "monocular" (boundary cells form a special case in their model). From the intracortical interaction and the fact that there are no constraints on arbors, one predicts that glabrous and dorsal bands of approximately 5 grid intervals each (±2 grid intervals about a central point) will become established[31]. This appears to be approximately consistent with the results seen[32]. In particular, because e→e connections are modifiable, squarish clumps of cells develop that are densely connected to one another by e→e synapses, but only weakly connected to other cortical cells by e→e synapses. Each clump is "monocular," responding to glabrous or to dorsal but not to both. Approximately 3 x 5 clumps form on the 12 x 28 non-boundary region of cortex, suggesting a linear clump size of between 4 and 5.5 grid intervals.

These clumps are termed "groups" by the authors, in part because each cell in a clump has an essentially identical receptive field. The authors argue that the formation of groups is the cause of the cortical organization observed in the model. We would argue, instead, that cortical organization develops in the model due to correlated inputs, intracortical interactions and a Hebbian type of learning rule. The groups are a possible *result* of such cortical organization that may be induced for particular choices of model parameters. One factor contributing to formation of groups may be that e→e synapses are assumed to be strongly dominant over thalamic inputs: e→e synapses are assigned 4.5 times the effectiveness of thalamic synapses for an equal synaptic strength. This may cause intracortical connections to

31. Note that the large periodicity, compared to the arbor size, suggests that some glabrous and dorsal sites may lose much of their input to cortex.

32. In examining pictures of the simulation, it is important to note that there are two excitatory cells at each grid position, but each is presented as though at a separate grid position. Thus pictures are presented with half the scale in one dimension as in the other dimension.

strongly dominate thalamic inputs in determining a cell's responses and cause a "clump" of strongly connected cells, developed by the Hebbian interactions, to become a "group" of identically responding cells.

Given an understanding of the sources of the model's behavior, a comparison to biology can be made. Two scales emerge from the model that can be compared with biology. One is the linear extent of the groups, which represents the scale of topographic disorder. On this scale, receptive fields appear to remain invariant across cortex, then to jump suddenly to a new location, so that the topographic map appears disorderly and discontinuous (see figure 8 of Pearson, Finkel and Edelman, 1987). The second scale is the linear extent of glabrous or dorsal patches. Our analysis demonstrates that these two scales must be roughly the same in the model, since both are determined identically by the intracortical interactions. This is true independently of the many details of the model and its implementation.

Somatosensory receptive fields are known to vary continuously and smoothly with distance across cortex over all distances larger than 50–100 microns (compare figure 3 of Stryker, Jenkins, and Merzenich, 1987 with figure 8 of Pearson, Finkel, and Edelman, 1987; also see Merzenich et al, 1987). Hence, the scale of topographic disorder represented by groups must be smaller than 100 microns. Yet dorsal patches typically are several or many 100's of microns in extent (Merzenich et al., 1987; Stryker, Jenkins, and Merzenich, 1987). The prediction, inherent in the process of group formation in the model, that topography should be disordered on the scale of dorsal patches as well as on the scale of the intracortical interactions[33], appears inconsistent with the biology.

33. A periodic scale determined by the intracortical interactions should be at least twice the horizontal extent over which cortical interactions are predominantly excitatory in the developing animal (the size will be larger than this if surrounding inhibitory interactions are relatively weak). The biological size of dorsal patches is likely to be consistent with this. In contrast, a scale of less than 50-100 microns, attributed by the model to the groups by identification of that scale with the biological scale of topographic disorder, seems likely not to be. Measurements of the intracortical interactions in the developing animal can provide an important independent check to the arguments made here.

The model is valuable in showing how the types of organization expected from a Hebbian mechanism can develop with a rather complex and detailed implementation of the Hebbian rule, and in applying these results to the somatosensory cortex. However, parameters that force groups to form may be precisely the wrong parameters, biologically. Rather, it seems likely that the cortical organization resulting from Hebbian interactions should develop in a way that allows smooth, continuous topographic variation of receptive fields across cortex.

More generally, we have shown that by simplifying a model, so that it incorporates only the simplest and best-established features of a system, and so that the essential factors responsible for its behavior can be understood, biological understanding may be deepened. While it is important to grapple with the realities of biological and biophysical complexity, a more complex model is not necessarily a more realistic one.

Conclusion

Ocular dominance segregation has provided perhaps the simplest and best characterized model of activity-dependent competition in neural development. We have shown that a minimal model of this process, incorporating only a competitive rule, correlations among inputs serving each eye, interactions across cortex, and limits to geniculocortical connectivity, is sufficient to account in surprising detail for much of the experimentally observed phenomena, as well as to predict the results of experiments yet undone. In particular, such a simple model is sufficient to predict the width of ocular dominance stripes to be expected from measurable biological parameters.

More detailed models will no doubt arise in the future that address the many features omitted from the current model. One would like to understand and incorporate more biophysical and temporal detail in modeling plasticity rules and geniculate and cortical activations. There are many classes of geniculate afferents, and the correlation between the activities of two afferents depends on the class to which each belongs (Mastronarde, 1989). Similarly, there are many classes of visual cortical cells (Lund, 1988; Martin, 1988). Initial geniculocortical and corticocortical connectivities are both more

specific and more stochastic than the simple distance-dependent rules we have used here (Lund, 1988; Martin, 1988). Cortex has three dimensions, not two. The retinotopic mapping to cortex is not linear, and the grid of retinal inputs is more nearly hexagonal than square, each of which could have important impacts on receptive field structure (Mallot, 1985; Soodak, 1987). The development of ocular dominance must be understood in the presence of orientation selectivity and other cortical properties. Sprouting and retraction of synapses may play a fundamental role, rather than a secondary role following physiological changes as assumed here. Better understandings of limitations on individual and total synaptic weights may be achieved in the future. Thus, the present model is only a beginning.

We believe nonetheless that this model can provide a framework for future endeavors. As one or another complexity is studied, one must ask whether it fundamentally alters or adds to the simple dynamics presented here, and if so how and why? The fact that so much of visual cortical development appears implicit in the simplest competitive dynamics makes plausible the idea that such simple dynamics may underlie the segregation that occurs amidst the complexity of the visual cortex.

Appendix

Derivation of the Model Equations From Nonlinear Rules

Consider a nonlinear version of the Hebb rule,

$$\frac{dS^L(x,\alpha,t)}{dt} = \lambda A(x-\alpha) f_c[c(x,t)] f_a[a^L(\alpha,t)] \qquad (A1)$$

(and similarly for S^R), with a nonlinear activation rule,

$$c(x,t) = g[\theta_x(t) + \sum_y B(x,y)\, c(y,t)] \qquad (A2)$$

where f_a, f_c and g are nonlinear functions and $\theta_x(t) = \sum_\beta [S^L(x,\beta,t)a^L(\beta,t) + S^R(x,\beta,t)a^R(\beta,t)]$. $c(x,t)$ is a function of all of the input strengths $\theta_y(t)$, although this is not indicated explicitly. We will see that the linearization of these equations can be taken to be of the form of eq. 5 for S^D.

The Hebb rule for the difference, $S^D(x,\alpha,t) \equiv S^L(x,\alpha,t) - S^R(x,\alpha,t)$ is now

$$\frac{dS^D(x,\alpha,t)}{dt} = \lambda A(x-\alpha) f_c[c(x,t)] f_a^D(\alpha,t) \tag{A3}$$

where $f_a^D(\alpha,t) \equiv f_a[a^L(\alpha,t)] - f_a[a^R(\alpha,t)]$. Let

$$S^S(x,\alpha,t) \equiv S^L(x,\alpha,t) + S^R(x,\alpha,t),$$

$$a^S(x,\alpha,t) \equiv a^L(x,\alpha,t) + a^R(x,\alpha,t),$$

$$a^D(x,\alpha,t) \equiv a^L(x,\alpha,t) - a^R(x,\alpha,t),$$

$$\theta_x^S(t) \equiv \tfrac{1}{2}\sum_\beta S^S(x,\beta,t)a^S(\beta,t),$$

$$\theta_x^D(t) \equiv \tfrac{1}{2}\sum_\beta S^D(x,\beta,t)a^D(\beta,t).$$

Then $\theta_x(t) = \theta_x^S(t) + \theta_x^D(t)$. Equation A3 will be expanded about $\theta_x^D(t) = 0$, to first order in $\theta_x^D(t)$.

Let $c^S(x,t)$ be the solution of

$$c^S(x,t) = g[\theta_x^S(t) + \sum_y B(x,y)\, c^S(y,t)]. \tag{A4}$$

Then

$$\frac{dS^D(x,\alpha,t)}{dt} \equiv \tag{A5}$$

$$\lambda A(x-\alpha) f_a^D(\alpha,t) \left\langle f_c[c^S(x,t)] + f'_c[c^S(x,t)] \sum_y \left.\frac{\partial c(x,t)}{\partial \theta_y(t)}\right|_{c\equiv c^S} \theta_y^D(t) \right\rangle + O[(\theta^D)^2].$$

Here f'_c is the derivative of the function f_c.

The partial derivative can be evaluated; letting $g'^S_x(t) \equiv g'[\theta_x^S(t) + \sum_y B(x,y)\, c^S(y,t)]$, where $'$ again indicates derivative, it is

$$\left.\frac{\partial c(x,t)}{\partial \theta_y(t)}\right|_{c\equiv c^S} = g'^S_x(t)\,[\mathbf{1} + \tilde{B} + (\tilde{B})^2 + \cdots]_{xy} \tag{A6}$$

where $\mathbf{1}$ is the identity matrix, $\tilde{B}$ is the matrix with elements $\tilde{B}_{xy} = B(x,y)g'^S_y(t)$, and $[...]_{xy}$ means the xy element of the matrix in brackets. Let $I(x,y,t) = [1 + B + (\tilde{B})^2 + \cdots]_{xy}$, $C(\alpha,\beta,t) = \tfrac{1}{2} f_a^D(\alpha,t) a^D(\beta,t)$, $D(x,t) = f'_c[c^S(x,t)] g'^S_x(t)$. Then eq. A5 becomes, to first order in θ^D,

$$\frac{\partial S^D(x,\alpha,t)}{\partial t} = \lambda A(x-\alpha) f_c[c^S(x,t)] f_a^D(\alpha,t) + \lambda A(x-\alpha) D(x,t) \sum_{y,\beta} I(x,y,t) C(\alpha,\beta,t) S^D(y,\beta,t). \tag{A7}$$

After averaging, by equality of the two eyes the first term must be zero. The lowest order term resulting from averaging of the second term is

$$\lambda A(x-\alpha) \sum_{y,\beta} \langle D(x,t) I(x,y,t) C(\alpha,\beta,t) \rangle \langle S^D(y,\beta,t) \rangle.$$

Suppose that $\langle D(x) I(x,y) C(\alpha,\beta) \rangle$ can be approximated by $\langle D(x) I(x,y) \rangle \langle C(\alpha,\beta) \rangle$. This will be true if the sum of the two eyes' inputs is statistically independent of the difference between the two eyes' inputs. By the assumption of homogeneity of cortex, $\langle D(x) I(x,y) \rangle$ can only depend on x–y, while $\langle C(\alpha,\beta) \rangle$ can only depend on $\alpha - \beta$. With

these assumptions, then, the linearized version of this nonlinear model is given by eq. 5 in the text for S^D.

References

Abraham, W.C., Gustafsson, B., and Wigstrom, H. (1987). Long-term potentiation involves enhanced synaptic excitation relative to synaptic inhibition in guinea-pig hippocampus. Journal of Physiology (London), 394:367-380.

Altmann, L., Luhmann, H.J., Greuel, J.M., and Singer, W. (1987). Functional and neuronal binocularity in kittens raised with rapidly alternating monocular occlusion. Journal of Neurophysiology, 58:965-980.

Anderson, P.A., Olavarria, J., and Van Sluyters, R.C. (1988). The overall pattern of ocular dominance bands in cat visual cortex. Journal of Neuroscience, 8:2183-2200.

Bienenstock, E.L., Cooper, L.N., and Munro, P.W. (1982). Theory for the development of neuron selectivity: Orientation specificity and binocular interaction in visual cortex. Journal of Neuroscience, 2:32-48.

Bishop, P.O., Henry, G.H., and Smith, C.J. (1971). Binocular interaction fields of single units in the cat striate cortex. Journal of Physiology (London), 216:39-68.

Blasdel, G.G. and Pettigrew, J.D. (1979). Degree of interocular synchrony required for maintenance of binocularity in kitten's visual cortex. Journal of Neurophysiology, 42:1692-1710.

Blasdel, G.G. and Salama, G. (1986). Voltage-sensitive dyes reveal a modular organization in monkey striate cortex. Nature, 321:579-585.

Brown, M.C., Jansen, J.K.S., and Van Essen, D. (1976). Polyneuronal innervation of skeletal muscle in new-born rats and its elimination during maturation. Journal of Physiology, 261:387-422.

Changeux, J.P. and Danchin, A. (1976). Selective stabilization of developing synapses as a mechanisms for the specification of neuronal networks. Nature, 264:705-712.

Chapman, B., Jacobson, M.D., Reiter, H., and Stryker, M.P. (1986). Ocular dominance shift in kitten visual cortex caused by imbalance in retinal electrical activity. Nature, 324:154-156.

Des Rosiers, M.H., Sakurada, O., Jehle, J., Shinohara, M., Kennedy, C., and Sokoloff, L. (1978). Demonstration of functional plasticity in the immature striate cortex of the monkey by means of the [14]C-deoxyglucose method. Science, 200:447-449.

Ferster, D. and LeVay, S. (1978). The axonal arborizations of lateral geniculate neurons in the striate cortex of the cat. Journal of Comparative Neurology, 182:923-944.

Fladby, T. and Jansen, J.K.S. (1987). Postnatal loss of synaptic terminals in the partially denervated mouse soleus muscle. Acta Physiologica Scandinavia, 129:239-246.

Fraser, S.E. (1980). Differential adhesion approach to the patterning of nerve connections. Developmental Biology, 79:453-464.

Gilbert, C.D. and Wiesel, T.N. (1983). Clustered intrinsic connections in cat visual cortex. Journal of Neuroscience, 3:1116-1133.

Griffith, W.H., Brown, T.H., and Johnston, D. (1986). Voltage-clamp analysis of synaptic inhibition during long-term potentiation in hippocampus. Journal of Neurophysiology, 55:767-775.

Guillery, R.W. (1972). Binocular competition in the control of geniculate cell growth. Journal of Comparative Neurology, 144:117-130.

Gustafsson, B., Wigstrom, H., Abraham, W.C., and Huang, Y.-Y. (1987). Long-term potentiation in the hippocampus using depolarizing current pulses as the conditioning stimulus to single volley synaptic potentials. Journal of Neuroscience, 7:774-780.

Hata, Y., Tsumoto, T., Sato, H., Hagihara, K., and Tamura, H. (1988). Inhibition contributes to orientation selectivity in visual cortex of cat. Nature, 335:815-817.

Hayes, W.P. and Meyer, R.L. (1988a). Retinotopically inappropriate synapses of subnormal density formed by misdirected optic fibers in goldfish tectum. Developmental Brain Research, 38:304-312.

Hayes, W.P. and Meyer, R.L. (1988b). Optic synapse number but not density is constrained during regeneration onto surgically halved tectum in goldfish: HRP-EM evidence that optic fibers

compete for fixed numbers of postsynaptic sites on the tectum. Journal of Comparative Neurology, 274:539-559.

Hayes, W.P. and Meyer, R.L. (1989a). Normal numbers of retinotectal synapses during the activity-sensitive period of optic regeneration in goldfish: HRP-EM evidence implicating synapse rearrangement and collaterral elimination during map refinement. Journal of Neuroscience, 9:1400-1413.

Hayes, W.P. and Meyer, R.L. (1989b). Impulse blockade by intraocular tetrodoxin during optic regeneration in goldfish: HRP-EM evidence that the formation of normal numbers of optic synapses and the elimination of exuberant optic fibers is activity independent. Journal of Neuroscience, 9:1414-1423.

Hebb, D.O. (1949). The Organization of Behavior. John Wiley and Sons, Inc., New York.

Hess, R., Negishi, K., and Creutzfeldt, O. (1975). The horizontal spread of intracortical inhibition in the visual cortex. Experimental Brain Research, 22:415-419.

Hubel, D.H. and Wiesel, T.N. (1962). Receptive fields, binocular interaction and functional architecture in the cat's visual cortex. Journal of Physiology, 160:106-154.

Hubel, D.H. and Wiesel, T.N. (1963). Receptive fields of cells in striate cortex of very young, visually inexperienced kittens. Journal of Neurophysiology, 26:994-1002.

Hubel, D.H. and Wiesel, T.N. (1965). Binocular interaction in striate cortex of kittens reared with artificial squint. Journal of Neurophysiology, 28:1041-1059.

Hubel, D.H. and Wiesel, T.N. (1970). The period of susceptibility to the physiological effects of unilateral eye closure in kittens. Journal of Physiology, 206:419-436.

Hubel, D.H. and Wiesel, T.N. (1972). Laminar and columnar distribution of geniculocortical fibers in the macaque monkey. Journal of Comparative Neurology, 146:421-450.

Hubel, D.H., Wiesel, T.N., and LeVay, S. (1977). Plasticity of ocular dominance columns in monkey striate cortex. Philosophical Transactions of the Royal Society of London Series B, 278:377-409.

Humphrey, A.L., Sur, M., Uhlrich, D.J., and Sherman, S.M. (1985a). Projection patterns of individual X- and Y-cell axons from the lateral geniculate nucleus to cortical area 17 in the cat. Journal

of Comparative Neurology, 233:159-189.

Humphrey, A.L., Sur, M., Uhlrich, D.J., and Sherman, S.M. (1985b). Termination patterns of individual X- and Y-cell axons in the visual cortex of the cat: Projections to area 18, to the 17/18 border region, and to both areas 17 and 18. Journal of Comparative Neurology, 233:190-212.

Kato, H., Bishop, P.O., and Orban, G.A. (1981). Binocular interaction on monocularly discharged lateral geniculate and striate neurons in the cat. Journal of Neurophysiology, 46:932-951.

Katz, L.C. & Constantine-Paton, M. (1988). Relationships between segregated afferents and postsynaptic neurons in the optic tectum of three-eyed frogs. Journal of Neuroscience, 8:3160-3180.

Keller, J.B. (1977). Effective behavior of heterogeneous media. In Landman, U. (Ed.), Statistical Mechanics and Statistical Methods in Theory and Application, pp. 631-644, Plenum.

Larson, J. and Lynch, G. (1986). Induction of synaptic potentiation in hippocampus by patterned stimulation involves two events. Science, 232:985-988.

Legendy, C.R. (1978). Cortical columns and the tendency of neighboring neurons to act similarly. Brain Research, 158:89-105.

LeVay, S. and Stryker, M.P. (1979). The development of ocular dominance columns in the cat. In Ferrendelli, J.A. (Ed.), Aspects of Developmental Neurobiology, pp. 83-98, Society for Neuroscience, Bethesda.

LeVay, S., Stryker, M.P., and Shatz, C.J. (1978). Ocular dominance columns and their development in layer IV of the cat's visual cortex: A quantitative study. Journal of Comparative Neurology, 179:223-244.

LeVay, S., Wiesel, T.N., and Hubel, D.H. (1980). The development of ocular dominance columns in normal and visually deprived monkeys. Journal of Comparative Neurology, 191:1-51.

Levick, W.R. and Williams, W.O. (1964). Maintained activity of lateral geniculate neurones in darkness. Journal of Physiology, 170:582-597.

Linsker, R. (1986a). From basic network principles to neural architecture: Emergence of spatial opponent cells. Proceedings of the National Academy of Sciences, 83:7508-7512.

Linsker, R. (1986b). From basic network principles to neural architecture: Emergence of orientation-selective cells. Proceedings of the National Academy of Sciences, 83:8390-8394.

Linsker, R. (1986c). From basic network principles to neural architecture: Emergence of orientation columns. Proceedings of the National Academy of Sciences, 83:8779-8783.

Lowel, S. and Singer, W. (1987). The pattern of ocular dominance columns in flat-mounts of visual cortex. Experimental Brain Research, 68:661-666.

Luhmann, H.J., Martinez Millan, L., and Singer, W. (1986). Development of horizontal intrinsic connections in cat striate cortex. Experimental Brain Research, 63:443-448.

Lund, J.S. (1988) Anatomical organization of macaque monkey striate visual cortex. Annual Review of Neuroscience, 11:253-288.

Mallot, H.A. (1985). An overall description of retinotopic mapping in the cat's visual cortex areas 17, 18, and 19. Biological Cybernetics, 52:45-51.

Malsburg, C. von der (1973). Self-organization of orientation sensitive cells in the striate cortex. Kybernetik, 14:85-100.

Malsburg, C. von der (1979). Development of ocularity domains and growth behavior of axon terminals. Biological Cybernetics, 32:49-62.

Malsburg, C. von der and Willshaw, D.J. (1976). A mechanism for producing continuous neural mappings: Ocularity dominance stripes and ordered retino-tectal projections. Experimental Brain Research, Supplement 1:463-469.

Malsburg, C. von der and Willshaw, D.J. (1977). How to label nerve cells so that they can interconnect in an ordered fashion. Proceedings of the National Academy of Sciences USA, 74:5176-5178.

Martin KA (1988). The Wellcome Prize lecture: From single cells to simple circuits in the cerebral cortex. Quarterly Journal of Experimental Physiology, 73:637-702.

Mastronarde, D.N. (1983a). Correlated firing of cat retinal ganglion cells. I. Spontaneously active inputs to X and Y cells. Journal of Neurophysiology, 49:303-324.

Mastronarde, D.N. (1983b). Correlated firing of cat retinal ganglion cells. II. Responses of X- and Y-cells to single quantal events.

Journal of Neurophysiology, 49:325-349.

Mastronarde, D.N. (1989). Correlated firing of retinal ganglion cells. Trends in Neurosciences, 12:75-80.

Merzenich, M.M., Nelson, R.J., Kaas, J.H., Stryker, M.P., Jenkins, W.M., Zook, J.M., Cynader, M.S., and Schoppmann, A. (1987). Variability in hand surface representations in areas 3b and 1 in adult owl and squirrel monkeys. Journal of Comparative Neurology, 258:281-296.

Miller, K.D. (1989a). Correlation-based models of neural development. In Gluck, M.A. and Rumelhart, D.E. (Eds.), Neuroscience and Connectionist Theory, Lawrence Erlbaum, Hillsboro, NJ.

Miller, K.D. (1989b). Orientation-selective cells can emerge from a Hebbian mechanism through interactions between ON- and OFF-center inputs. Society for Neuroscience Abstracts, 15:794.

Miller, K.D. (1989c). Ph. D. Thesis, Stanford University Medical School. University Microfilms, Ann Arbor.

Miller, K.D., Keller, J.B., and Stryker, M.P. (1986). Models for the formation of ocular dominance columns solved by linear stability analysis. Society for Neuroscience Abstracts, 12:1373.

Miller, K.D., Keller, J.B., and Stryker, M.P. (1989). Ocular dominance column development: Analysis and simulation. Science, 245:605-615.

Murray, M., Sharma, S., and Edwards, M.A. (1982). Target regulation of synaptic number in the compressed retinotectal projection of goldfish. Journal of Comparative Neurology, 209:374-385.

Nicoll, R.A., Kauer, J.A., and Malenka R.C. (1988). The current excitement in long-term potentiation. Neuron, 1, 97-103.

Ohzawa, I. and Freeman, R.D. (1986). The binocular organization of simple cells in the cat's visual cortex. Journal of Neurophysiology, 56:221-242.

Oja, E. (1982). A simplified neuron model as a principal component analyzer. Journal of Mathematical Biology, 15:267-273.

Pearson, J.C., Finkel, L.H., and Edelman, G.M. (1987). Plasticity in the organization of adult cerebral cortical maps: A computer simulation based on neuronal group selection. Journal of Neuroscience, 7:4209-4223.

Rakic, P. (1977). Prenatal development of the visual system in the rhesus monkey. Philosophical Transactions of the Royal

Society of London Series B, 278:245-260.

Reiter, H.O. and Stryker, M.P. (1988). Neural plasticity without postsynaptic action potentials: Less-active inputs become dominant when kitten visual cortical cells are pharmacologically inhibited. Proceedings of the National Academy of Sciences USA, 85:3623-3627.

Reiter, H.O., Waitzman, D.M., and Stryker, M.P. (1986). Cortical activity blockade prevents ocular dominance plasticity in the kitten visual cortex. Experimental Brain Research, 65:182-188.

Rodieck, R.W. and Smith, P.S. (1966). Slow dark discharge rhythms of cat retinal ganglion cells. Journal of Neurophysiology, 29:942-953.

Rose, G.M. and Dunwiddie, T.V. (1986). Induction of hippocampal long-term potentiation using physiologically patterned stimulation. Neuroscience Letters, 69:244-248.

Schneider, G.E. (1973). Early lesions of superior colliculus: Factors affecting the formation of abnormal retinal projections. Brain, Behavior and Evolution, 8:73-109.

Sejnowski, T.J. (1977). Storing covariance with nonlinearly interacting neurons. Journal of Mathematical Biology, 4:303-321.

Senden, Marius von (1960). Space and Sight; the Perception of Space and Shape in the Congenitally Blind Before and After the Operation. Translated by P. Heath. Free Press, Glencoe, Ill.

Shatz, C.J., Lindstrom, S., and Wiesel, T.N. (1977). The distribution of afferents representing the right and left eyes in the cat's visual cortex. Brain Research, 131:103-116.

Shatz, C.J. and Stryker, M.P. (1978). Ocular dominance in layer IV of the cat's visual cortex and the effects of monocular deprivation. Journal of Physiology, 281:267-283.

Sherman, S.M., Guillery, R.W., Kaas, J.H., and Sanderson, K.J. (1974). Behavioral, electrophysiological, and morphological studies of binocular competition in the development of the geniculocortical pathways of cats. Journal of Comparative Neurology, 158:1-18.

Sherman, S.M. and Spear, P.D. (1982). Organisation of visual pathways in normal and visually deprived cats. Physiological Review, 62:738-855.

Singer, W. (1985). Central control of developmental plasticity in the

mammalian visual cortex. Vision Research, 25:389-396.

Soodak, R.E. (1987). The retinal ganglion cell mosaic defines orientation columns in striate cortex. Proceedings of the National Academy of Sciences USA}, 84:3936-3940.

Stent, G.S. (1973). A physiological mechanism of Hebb's postulate of learning. Proceedings of the National Academy of Sciences USA, 70:997-1001.

Stryker, M.P. (1986). The role of neural activity in rearranging connections in the central visual system. In Ruben, R.J., Water, T.R. Van De, and Rubel, E.W. (Eds.), The Biology of Change in Otolaryngology, pp. 211-224, Elsevier Science B.V., Amsterdam.

Stryker, M.P. and Harris, W. (1986). Binocular impulse blockade prevents the formation of ocular dominance columns in cat visual cortex. Journal of Neuroscience, 6:2117-2133.

Stryker, M.P., Jenkins, W.M., and Merzenich, M.M. (1987). Anesthetic state does not affect the map of the hand representation within area 3b somatosensory cortex in owl monkey. Journal of Comparative Neurology, 258:297-303.

Swindale, N.V. (1980). A model for the formation of ocular dominance stripes. Proceedings of the Royal Society of London Series B., 208:243-264.

Swindale, N.V. (1988). Role of visual experience in promoting segregation of eye dominance patches in the visual cortex of the cat. Journal of Comparative Neurology, 267:472-488.

Swindale, N.V., Matsubara, J.A., and Cynader, M.S. (1987). Surface organization of orientation and direction selectivity in cat area 18. Journal of Neuroscience, 7:1414-1427.

Toyama, K., Kimura, M., and Tanaka, K. (1981a). Cross-correlation analysis of interneuronal connectivity in cat visual cortex. Journal of Neurophysiology, 46:191-201.

Toyama, K., Kimura, M., and Tanaka, K. (1981b). Organization of cat visual cortex as investigated by cross-correlation technique. Journal of Neurophysiology, 46:202-214.

Tso, D.Y., Gilbert, C.D., and Wiesel, T.N. (1986). Relationships between horizontal interactions and functional architecture in cat striate cortex as revealed by cross correlation analysis. Journal of Neuroscience, 6:1160-1170.

Tusa, R.J., Palmer, L.A., and Rosenquist, A.C. (1978). The

retinotopic organization of area 17 (striate cortex) in the cat. Journal of Comparative Neurology, 177:213-235.

Van Sluyters, R.C. and Levitt, F.B. (1980). Experimental strabismus in the kitten. Journal of Neurophysiology, 43:686-699.

Whitelaw, V.A. and Cowan, J.D. (1981). Specificity and plasticity of retinotectal connections: A computational model. Journal of Neuroscience, 1:1369-1387.

Wiesel, T.N. and Hubel, D.H. (1963a). Single-cell responses in striate cortex of kittens deprived of vision in one eye. Journal of Neurophysiology, 26:1003-1017.

Wiesel, T.N. and Hubel, D.H. (1963b). Effects of visual deprivation on morphology and physiology of cells in the cat's lateral geniculate body. Journal of Neurophysiology, 26:978-993.

Wiesel, T.N. and Hubel, D.H. (1965). Comparison of the effects of unilateral and bilateral eye closure on cortical unit responses in kittens. Journal of Neurophysiology, 28:1029-1040.

Wiesel, T.N., Hubel, D.H., and Lam, D.M.K. (1974). Autoradiographic demonstration of ocular dominance columns in the monkey striate cortex by means of transneuronal transport. Brain Research, 79:273-279.

Willshaw, D.J. and Malsburg, C. von der (1976). How patterned neural connections can be set up by self-organization. Proceedings of the Royal Society of London Series B, 194:431-445.

Willshaw, D.J. and Malsburg, C. von der (1979). A marker induction mechanism for the establishment of ordered neural mappings: Its application to the retinotectal problem. Philosophical Transactions of the Royal Society of London Series B, 287:203-243.

Worgotter, F. and Eysel, U. Th. (1989). On the influence and topography of excitation and inhibition at orientation-specific visual cortical neurons in the cat. Submitted for publication.